

# Sensitivity of Motor Adaptation to the Statistical Properties of an Environmental Load

Timothy Michael Haswell  
*Marquette University*

---

## Recommended Citation

Haswell, Timothy Michael, "Sensitivity of Motor Adaptation to the Statistical Properties of an Environmental Load" (2010). *Master's Theses (2009 -)*. Paper 44.  
[http://epublications.marquette.edu/theses\\_open/44](http://epublications.marquette.edu/theses_open/44)

**SENSITIVITY OF MOTOR ADAPTATION TO THE STATISTICAL  
PROPERTIES OF AN ENVIRONMENTAL LOAD**

by

Timothy M Goetz-Haswell, B.S.

A Thesis submitted to the Faculty of the Graduate School,  
Marquette University,  
in Partial Fulfillment of the Requirements for  
the Degree of Master of Science

Milwaukee, Wisconsin

May 2010

**ABSTRACT**  
SENSITIVITY OF MOTOR ADAPTATION TO THE STATISTICAL  
PROPERTIES OF AN ENVIRONMENTAL LOAD

Timothy M Goetz-Haswell, B.S.

Marquette University, 2010

Linear, limited-memory models capture many important features of adaptive motor performance during reaching, stepping and pointing. A recent study in our lab found that a model fitted to data obtained from subjects reaching against elastic loads which varied from trial-to-trial later failed to fit the steady-state response behavior of subjects exposed to deterministic, step changes in load. Does motor adaptation depend on statistical properties of the environment (eg. mean load strength and variability)? Neurologically intact volunteers (n=14) made 6 blocks of 100 planar, ballistic, 10cm, out-and-back reaching movements against spring-like loads having equilibrium positions at the hand's starting point. View of the limb was not allowed. Load stiffness varied trial-by-trial, and each block of movements differed in mean and/or variance such that three, 3-block contrasts were evaluated: increasing standard deviation (VAR), increasing mean (MEAN), and proportionally increasing standard deviation and mean (WEBER). In the VAR and MEAN contrasts, either the mean or the standard deviation of the load stiffness sequence was held constant while the other parameter varied systematically. In WEBER contrast, mean and standard deviation scaled proportionally over the contrast. The zero location of the transfer function moved toward the origin as variability increased. This trend in the zero location was the result of an unbalance in the decrease in the influence of previous load and the decrease of effective limb compliance with increasing variability. Specifically, the decrease in the influence of prior load was greater than the decrease in effective limb compliance. Effective limb compliance decreased to a larger extent in the MEAN and WEBER contrasts, which both presented an increase in mean load. In the MEAN contrast, the decrease in effective limb compliance with increasing mean load was balanced by an equivalent decrease in the influence of prior load, resulting in no significant change in the transfer function zero location. No changes in the influence of prior errors were observed in any of the contrasts. Thus, motor adaptation adjusts in two ways: the influence of prior load on subsequent movements decreases both when the environment is more variable and when effective limb compliance decreases with the mean load.

## ACKNOWLEDGEMENTS

Timothy M Goetz-Haswell, B.S.

I would like to thank my advisor Dr Robert A Scheidt for allowing me this great opportunity to challenge myself and for his guidance and patience with me as I made my way through this process. I have learned so much, thank you.

I would like to thank my thesis committee members Drs Brian D Schmit and Jack M Winters for their exceptional feedback and insight.

I would also like to thank my wife Wendy for her love, support, and patience. You have helped me more than you may know.

## TABLE OF CONTENTS

ACKNOWLEDGEMENTS .....	i
TABLE OF FIGURES .....	iv
CHAPTER	
I. RATIONALE AND SPECIFIC AIMS.....	1
II. BACKGROUND AND SIGNIFICANCE.....	4
Adaptive Motor Responses to Changing Environmental Loads .....	4
Motor Adaptation: A Bayesian Perspective .....	7
Physiological Mechanisms Contributing to Motor Adaptation .....	12
Computational Models of Motor Adaptation.....	14
III. RESEARCH METHODS.....	17
Data Collection.....	18
Experimental Protocol .....	19
Data Analysis .....	25
Statistical Hypothesis Testing.....	28
EMG Analysis .....	29
Fatigue Assessment.....	29
IV. RESULTS .....	31
Adaptation Model Structure Selection .....	33
Effect of Environmental Variability on Motor Command Updating .....	35
Effect of Mean Environmental Load on Motor Command Updating.....	36
Effect of ‘Weber-Equivalent’ Load on Motor Command Updating.....	39
Lateral Forces Against the Stiff Controller .....	41
Effect of Multifactor Correlation on Model Fit.....	42
Average EMG Trends by Contrast Level.....	43

Fatigue .....	45
V. DISCUSSION.....	47
Zero Location Changes with the Variability of the Load .....	49
Pole Location ( $a_1$ ) Does Not Vary With Load.....	50
The Role of Limb Compliance in Reach Accuracy.....	52
Reject Weber Equivalency .....	53
Effects of Variability in Other Load Properties .....	55
VI. CONCLUSIONS AND FUTURE DIRECTIONS.....	56
Conclusions.....	56
Future Directions .....	57
REFERENCES.....	60

## TABLE OF FIGURES

<u>Figure 1</u> : Diagrammatic Representation of the Mechanical Environment.....	20
<u>Figure 2</u> : Histograms of stiffness distributions for experimental blocks.....	23
<u>Figure 3</u> : Autocorrelation values for the load stiffness series of each block of trials. ....	24
<u>Figure 4</u> : Kinematic and kinetic time series.....	32
<u>Figure 5</u> : Average across subjects of peak displacement and displacement at peak velocity and peak acceleration by block. ....	33
<u>Figure 6</u> : Average kinematic error by binned load stiffness values across subjects.....	34
<u>Figure 7</u> : Average adaptation model parameters for the VAR (increasing load variability) contrast across subjects.....	35
<u>Figure 8</u> : Average adaptation model parameters for the MEAN (increasing mean load) contrast across subjects.....	37
<u>Figure 9</u> : Average adaptation model parameters for the WEBER (simultaneously increasing load mean and variability) contrast across subjects. ....	39
<u>Figure 10</u> : Lateral forces applied by subjects against the stiff controller. ....	42
<u>Figure 11</u> : Raw and average EMG traces scaled as a percentage of MVC. ....	45
<u>Figure 12</u> : Average change in EMG to Force ratio for “effort test” trials relative to an initial “effort test” trial conducted prior to the first block of trials. ....	46
<u>Figure 13</u> : Step and impulse response plots for a selection of zero location values.....	50

## RATIONALE AND SPECIFIC AIMS

Motor adaptation is an important form of learning whereby trial-by-trial adjustments are made to motor commands in order to recover some desired performance despite persistent perturbation or change in load. Systems identification techniques have been used to characterize motor adaptation (Bock 2003; Conditt et al. 1997; Lai et al. 2003; Scheidt et al. 2005; Scheidt et al. 2001), finding that a linear, limited memory model captures many important features of the adaptive response (Scheidt et al. 2005; Scheidt et al. 2001). This model has a form identical to that of an infinite impulse response (IIR) filter used in signal processing applications. Very recently, Scheidt and colleagues have demonstrated that the impulse response properties of motor adaptation vary depending on the sensory context within which adaptation takes place (Scheidt et al. 2005). Here we seek to determine whether the response properties of this adaptation also depend on the statistical properties of the environment, namely the mean strength of load and its variability.

Lai et al. (2003) have examined how the extent of motor adaptation varies with the magnitude of environmental perturbations. Although their assessment of adaptation showed some variation over the five perturbation levels tested, this trend was not found to be statistically significant. This equivocal outcome likely occurred because the range of perturbation strengths was too limited to evoke movement errors that varied systematically with load condition.

A recent study conducted in our lab has characterized the motor adaptive response to elastic loads that vary randomly from one trial to the next (Judkins 2004). A limited-memory model of sensorimotor adaptation derived from trials with unpredictable loads fit

the transient response behavior of hand path errors with fidelity. However, these same models failed to fit steady-state errors when subjects were exposed to deterministic, step changes in load. Since a step change in load is very predictable after the initial impulse, it is possible that subjects may have adopted different adaptive strategies depending on the statistical properties of the load. For example, when reaching against a highly predictable perturbing force (low variability), performance errors likely reflect variability and/or errors in motor planning which should be compensated for on subsequent movement attempts. In contrast, when reaching against an unpredictable loads (i.e. environments with high variability), performance errors may reflect errors induced by the changing load to a greater extent than errors in motor planning. We propose to evaluate whether and how subjects alter their motor adaptation strategy depending on the statistical properties of the mechanical load.

Since motor adaptation is driven by sensory inputs, it may be necessary to consider the role of sensory-perception processing in motor adaptation. It has long been known that neurosensory mechanisms are sensitive to the statistical properties of environmental stimuli. Weber's law, a central tenet of the study of human sensation and perception (psychophysics), states that for a particular amplitude of a given stimulus ( $I_0$ ), the following stimulus ( $I_1$ ) must increase (or decrease) by a constant proportion ( $k$ ) of the original stimulus level to bring about a just noticeable difference (jnd) in sensation (Weber, 1978; Gescheider 1985; Matlin and Foley 1997):

$$\frac{\Delta I}{I_0} = \frac{I_1 - I_0}{I_0} = k \quad (1)$$

(Note that  $k$  is unitless.) If the sensory mechanisms contributing to motor adaptation are subject to similar neuro-physiological constraints giving rise to Weber's law, then sets of pseudorandom stiffness loads whose mean and standard deviations scale by a constant ratio will be perceived as having similar distributions, thus giving rise to similar trial-by-trial adaptations. We propose to test this hypothesis by comparing adaptation models derived from sets of loads having carefully selected statistical properties. Specifically, our aims are:

- 1) To test the hypothesis that the sensorimotor information processing leading to motor adaptation is sensitive to statistical properties of the environmental load, and
- 2) To test the hypothesis that sensorimotor information processing serving motor adaptation adheres to Weber's Law for sensation.

We expect the experimental results will increase our understanding of how recent experience shapes motor performance. This knowledge will likely be necessary for improving practice-based therapies promoting recovery from motor impairments following injury to the neuromotor pathways (e.g. stroke).

## BACKGROUND AND SIGNIFICANCE

This section will review the core research motivating this study. This study focuses specifically on motor adaptation, which we differentiate from visuomotor adaptation in that this work is conducted in the absence of concurrent visual feedback. This makes the experimental task adaptations localized to the proprioceptive sensory and motor systems as opposed to the visuomotor system. This allows us to focus on the use of proprioception as it applies to planning of movements performed without concurrent visual feedback and removes complicating and conflicting factors such as visuospatial transformations, the proportions of visual and proprioceptive contributions to feedforward planning of movement, and attention paid to visual feedback. We will also briefly discuss the relation of the motor adaptive process to Bayesian processes and how Weber's Law, as interpreted by L. L. Thurstone (Thurstone 1927), complies with Bayes' Theorem.

### ***Adaptive Motor Responses to Changing Environmental Loads***

Motor adaptation is an iterative process by which deviations in movement caused by some perturbation or load are reduced over a number of repetitions in an attempt to regain a level of performance similar to that occurring prior to introduction of the perturbation or load. Many types of load have been evaluated experimentally and have been shown to be compatible with this process, demonstrating that it is a robust mechanism for correcting motion. Motor adaptation appears to be able to compensate for position-, velocity-, and acceleration-dependant dynamic loads (stiffness (Weeks et al. 1996), viscous/viscous-curl (Hannaford et al. 1984; Lai et al. 2003; Scheidt et al. 2001; Scheidt et al. 2000), and inertia

(Sainburg et al. 1999), respectively) and combinations thereof. However, there is evidence that one cannot adapt to time-dependant dynamic loads per se but rather that the motor system appears to "learn" such loads via a kinematics-dependant approximation (Conditt et al. 1997). The internal sense of limb kinematics (termed proprioception) clearly plays a role in motor adaptation. Research has demonstrated that most people will rely on vision if it is available, suggesting that it is believed to be more accurate and/or reliable. However, evidence indicates that vision is not necessary for adaptation (Conditt et al. 1997; Sainburg et al. 1999; Scheidt et al. 2005; Scheidt et al. 2001; Scheidt et al. 2000). This indicates that proprioception is a sufficient sensory input for motor adaptation.

Proprioceptive sensory information can come from a number of different sensory organs in the skin, joints, and muscles. Typically, muscle spindles are assumed the primary sensory organ responsible for the transduction of length and length change in extrafusal (voluntary) muscle. Two related sensory organs comprise muscle spindles – the nuclear bag fiber and the nuclear chain fiber. The nuclear bag fibers are named for their bulged central region that contains most of the nuclei of their constituent cells. These fibers are very sensitive to the rate of length change and their response is transmitted to the CNS on group Ia (primary) afferents. Nuclear chain fibers are shorter and thinner than nuclear bag fibers and get their name from the single-file arrangement of their nuclei. Nuclear chain fibers vary their firing rate in proportion to the length of the muscle. Nuclear chain fibers transmit their signals on both group Ia (primary) and group II (secondary) afferents. During rapid length changes, the response of the nuclear bag fibers obscures the response of the nuclear chain fibers on the primary afferent as it is much larger. These organs contain their own contractile elements (intrafusal muscle fibers) that are innervated by  $\gamma$ -motor efferent neurons. These  $\gamma$ -motor efferent pathways appear to have activity proportional to the

primary ( $\alpha$ -) motor efferent activity directed to the extrafusal muscle fibers (Granit, 1975; Guyton and Hall 2000; Hulliger and Prochazka, 1983). Some have proposed that the central nervous system (CNS) controls the sensitivity of muscle spindles by changing the "gain" of the  $\gamma$ -motor drive relative to the  $\alpha$ -motor drive (Prochazka et al. 1985), leading to a disparity in the length change of the spindle relative to the surrounding extrafusal muscle fibers. This causes the spindle length to deviate from its normal resting length increasing its firing rate in the case of an elongated spindle and reducing sensitivity in the reverse case. Ribot-Cisar *et al* (2000) conducted a microneurographical study of passive human ankle movements attempting to train subjects to adjust their  $\gamma$ -motor drive. The subjects could only reduce  $\gamma$ -motor drive through focused whole-body relaxation and these efforts were disrupted by mental computation. Other studies have not uncovered any greater successes in voluntary  $\gamma$ -efferent control (Gandevia et al. 1997; Kakuda et al. 1997) despite success in training animals to change  $\gamma$ -motor drive signals (Gandevia and Burke 1985) and observations that a number of external stimuli can give rise to changes in spindle activation threshold (Burke et al. 1980). These findings suggest that either humans have poor voluntary control of  $\gamma$ -motor drive or that much more practice is required to gain this voluntary control (given that animal studies use much more extensive training than human studies).

While force feedback, from Golgi tendon organs or hand mechanoreceptors, may be involved in motor adaptation, rapid minimization of applied force does not appear to be the principle factor driving motor adaptation in reaching tasks with position goals. A reaching study by Scheidt *et al* (2000) demonstrated that subjects continue to generate similar corrective forces to those needed to compensate for an adapted perturbing load when they continue to experience a mechanical resistance to their efforts even if those forces no longer have the same dynamics of the adapted perturbation. In this study, subjects adapted to a

perturbing load, then a stiff controller was enabled that held them to their desired straight-line-reach path. Subjects were not directly notified of this change and continued to generate similar forces against the new load and exhibited only a slow decay in corrective force production. This decay had a time constant more than 16 times greater than that observed in subjects returning to their unperturbed kinematics while interacting with a passive manipulandum (Scheidt et al. 2000). This suggests that humans are not likely to make large changes to their motor commands if their efforts do not result in large over-compensatory movements. It does not appear that the sense of the applied force is particularly sensitive to the dynamics of the perturbing force given that subjects do not quickly realize that the new force field is assisting them in making straight reaches. This evidence suggests that, while force output is a motor plan parameter that is adjusted in adaptation during horizontal planar reaching, the appropriateness of the force output is determined by kinematic (most likely positional) deviations from the intended path. From these findings, if force information is used in human motor planning, then it has a much larger time constant than that applied to positional feedback.

### ***Motor Adaptation: A Bayesian Perspective***

Some researchers have proposed that motor adaptation can be modeled using a Bayesian conceptual framework (Bays and Wolpert 2007; Burge et al. 2008; Kording et al. 2007; Korenberg and Ghahramani 2002; Krakauer et al. 2006; Wei and Kording 2009; Wolpert 2007). The models they have proposed are similar in structure to existing models in that they typically use kinematic error and occasionally perturbation or load strength with very limited memory to estimate model parameters. However, these models estimate the

variance of certain noise sources such as sensory noise and execution noise and are fit by maximizing probability, rather than minimizing error.

Bayes' Theorem guides the underlying logic for Bayesian models. This theorem describes the update of probability based on new information.  $P(H|E)$  is the new (or posterior) probability of hypothesis  $H$  given new evidence  $E$ ,  $P(H)$  is our original (or prior) estimate of the probability of hypothesis  $H$ ,  $P(E|H)$  represents the likelihood of "seeing" the new information  $E$  assuming we are correct in our assumption of the value of  $H$ , and  $P(E)$  is the sum of all possible products  $P(E|H_i)P(H_i)$  for every possible hypothesis  $H_i$ , called the marginal probability. The marginal probability ensures that the probabilities for all hypotheses  $H_i$  sum to 1. The determination of the posterior probability  $P(H|E)$  allows us to update our belief of the probability of our hypothesis  $H$  given the new information  $E$  and this can be done iteratively by setting the prior probability  $P(H)$  equal to the posterior probability estimate  $P(H|E)$  and calculate a new posterior probability each time new information  $E$  is made available.

In the case of motor adaptation, one can have a hypothesis of a particular environmental load magnitude ( $H$ ) and update that hypothesis ( $P(H|E)$ ) using measurement estimates ( $E$ ) gleaned from reaches made in the environment in the form of movement (e.g. reach extent, lateral deviation, etc.) error or a sense of effort (e.g. efference copy, Golgi tendon organ information, etc.) (Wei and Kording 2009; Wolpert 2007).

$$P(H|E) = \frac{P(E|H)P(H)}{P(E)} = \frac{P(E|H)P(H)}{\sum_{i=0}^n P(E|H_i)P(H_i)} \quad (2)$$

A number of researchers (Burge et al. 2008; Korenberg and Ghahramani 2002; Todorov 2005; Wolpert 2007) have proposed the use of an extension of Bayes' Theorem

know as a Kalman filter to model the motor adaptive process. The Kalman filter attempts to determine the true value of some input signal by estimating the probability that each measurement of that signal is correct rather than corrupted by noise. To do this, the variability of the noise and the variability of true signal are estimated recursively as each new measurement becomes available. If the noise has stationary statistical properties, the filter will converge on an estimate of these properties and provide a very good estimate of the true signal.

The Kalman filter is implemented as a series of equations that can generally be divided into “prediction” and “correction” groupings (Maybeck 1979; Welch and Bishop 2006). The prediction equations (3) and (4) form a prediction ( $\hat{x}_i^-$ ) of the measurement ( $z_i$ ) that will be made on the next time step ( $i$ ) and the variance of the signal ( $\sigma_i^{2-}$ ) using the existing estimates of the true value of the signal being measured ( $\hat{x}_{i-1}$ ) and the statistics of the signal ( $\sigma_{i-1}^2$ ). The correction equations (5), (6), and (7) update the estimates of the true signal ( $\hat{x}_i$ ) and its variance ( $\sigma_i^2$ ) in light of the new measurement ( $z_i$ ), and the process repeats. In these equations,  $A$  and  $B$  are the coefficients of the difference equation (3) that describe the relationship between the signal of interest ( $\hat{x}_i$ ) and an (optional) input signal ( $u_{i-1}$ ). The Kalman gain ( $K$ ) controls the influence of the measurement residual, or prediction error, ( $z_i - \hat{x}_i^-$ ) on the update of the estimation of the true signal ( $\hat{x}_i$ ) in (6). The Kalman gain is calculated in (5) from the ratio of the predicted variance of the input signal ( $\sigma_i^{2-}$ ) and the variance of the noise in the measurement ( $\sigma_z^2$ ), which is the step that make the Kalman filter a Bayesian estimator. Typically, the variance of the measurement noise ( $\sigma_z^2$ ) can be determined empirically before its use in the Kalman filter. The  $\sigma_{process}^2$  term

represents a guess at the variance of the signal of interest and is usually not critical because it is recursively adjusted in (4).

**Kalman Filter Prediction Equations:**

$$\hat{x}_i^- = A\hat{x}_{i-1} + Bu_{i-1} \quad (3)$$

$$\sigma_i^{2-} = A\sigma_{i-1}^2 A^T + \sigma_{process}^2 \quad (4)$$

**Kalman Filter Correction Equations:**

$$K_i = \frac{\sigma_i^{2-}}{\sigma_i^{2-} + \sigma_z^2} \quad (5)$$

$$\hat{x}_i = \hat{x}_i^- + K_i(z_i - \hat{x}_i^-) \quad (6)$$

$$\sigma_i^2 = (I - K_k)\sigma_i^{2-} \quad (7)$$

An example of the use of a Kalman filter for modeling motor adaptation can be found in the work of Burge et. al. (2008). These researchers used a Kalman filter to model the visuomotor adaptation of subjects reaching without concurrent visual feedback, but receiving feedback of reach end point. The measured signal ( $z$ ) was reach end point error and the output ( $\hat{x}$ ) was an estimation of the magnitude of the visuomotor mapping that the researchers applied to the visual feedback presented to the subject. The imposed visuomotor mapping in this case was a displacement between the true reach end point and the corresponding visual feedback of the reach end point. Burge et. al. manipulated the measurement uncertainty ( $\sigma_z^2$ ) by blurring the visual feedback with a zero-mean Gaussian distribution with standard deviation  $\sigma_{blur}$ . They used a visual discrimination task prior to the reaching experiment to empirically measure  $\sigma_z^2$  for each blurring magnitude ( $\sigma_{blur}$ ). They also manipulated visuomotor mapping uncertainty ( $\sigma^2$ ) by adding a random walk with a standard deviation  $\sigma_{walk}$  to the step change in visuomotor mapping they used to probe the adapting subjects. Note that a random walk is a set of values created by iteratively adding a

value taken from a random distribution (in this case a zero-mean, Gaussian-distribution) to the previous value in the set, creating a randomly varying, but autocorrelated set of values. They found that as they increased  $\sigma_{blur}$ , increasing measurement uncertainty  $\sigma_z^2$  in viewing the reach end point feedback, the convergence toward the true visuomotor mapping (adaptation rate) slowed. They also found when  $\sigma_{walk}$  was increased, increasing the variability of the measured signal (the visuomotor mapping), the estimated visuomotor mapping changed more rapidly (adaptation rate increased). Since subjects' behavior was well described by the Kalman filter, the interpretation was that when  $\sigma_{blur}$  is high, subjects “trust” the measurement (visual feedback) less and do not allow visual feedback to change the estimated visuomotor mapping quickly. When  $\sigma_{walk}$  was increased, the visuomotor mapping uncertainty ( $\sigma^2$ ) increased and reach end point errors in the visual feedback were “trusted” because the visuomotor mapping was likely to vary.

In Bayesian models, the variance of the estimated noise controls the responsiveness of the model parameter update. Specifically, when the magnitude of new input data is improbable given the current model parameter and noise variance estimates, its contribution to the model parameter estimates is minimized and the noise estimate is adjusted. After several trials, as the noise estimate becomes accurate, the model parameter estimates obtain good noise rejection. The interpretation is that if environmental variability is small (i.e. within the range of intrinsic sensorimotor variability), then systematic errors (like a bias toward over-reaching) are likely the result of motor command errors and should be corrected. If environmental variability is large, then errors are likely to be variable rather than systematic and due, in large part, to this high environmental variability rather than an error in the motor command. This variability may also make it difficult to determine the

contribution of motor command error to the total error. In the experiments we describe in this report, we will model the responses of human subjects to changes in environmental load variability and mean load strength. In doing so, we are exploring whether or not motor adaptation might be described as optimal, in the sense that it adheres to Bayes' Theorem.

### ***Physiological Mechanisms Contributing to Motor Adaptation***

Psychophysics is the area of research concerned with characterizing the relationships between sensation, perception and action. Sensation refers to the act of translating (i.e. transducing) stimulus energy into neural signals, perception refers to the detection of the sensed stimulus and the formation of a mental representation of its magnitude and action refers to the generation of a physical response to the stimulus. Determining a mathematical relationship between these concepts has long been a goal of the motor control community. Some of these efforts have given rise to models such as Weber's Law, the Weber-Fechner Law, and the Stevens Power Law, which make use of another concept termed "just noticeable difference" or "jnd". The jnd can be thought of as the 'resolution' of perception, in that it describes how much the stimulus intensity needs to change (relative to a control condition) in order that a difference is perceptible. From his work, Weber found (for the stimuli he studied) that the magnitude of a stimulus change must increase by a constant proportion of the initial (control) intensity to elicit a jnd regardless of control magnitude. This constant proportion has come to be known as the Weber fraction  $k = \frac{\Delta I}{I}$ , where  $I$  is a given stimulus intensity and  $\Delta I$  is the change in stimulus intensity necessary to elicit a "jnd" (Weber, 1978; Gescheider 1985; Matlin and Foley 1997). Perception of many different

sensory stimuli has been found to conform to this basic relationship, although different constants ( $k$ ) are associated with the different sensory stimuli (Gescheider 1985).

Weber's Law can be viewed as a discrete empirical model of a continuous statistical process. In his experiments and others like them, the just-noticeable-difference (jnd) was assigned some fixed probability, typically 75% chance of correctly detecting a stimulus change. In doing so, Weber and others were essentially asking their subjects to perform a sensory-perceptive t-test with an alpha level of 0.25, discretizing the continuous process into a true-false response. This view is by no means a new one, in fact it was proposed in 1927 by L. L. Thurstone (Thurstone 1927). Thurstone proposed that Weber's Law is a simplification of the real continuous discriminatory process that was occurring since the laws used a fixed detection threshold. Noise exists in all sensory inputs to varying degrees depending on the environment. Nevertheless, the sensory system appears quite capable of discriminating useful information from the noise despite potential non-stationarity of that environmental noise. The dependence of perception on stimulus intensity as described by Weber's Law is likely a result of the increasing difficulty in discriminating differences in sensory information subject to signal-dependent noise, as has been demonstrated in the visual system (Todorov 2005). Given the broad application of Weber's Law, we hypothesize that signal-dependent noise sources in the motor system may also contribute to the observation of a similar scaling relationship in the way subjects respond as they adapt to blocks of trial-by-trial varying loads of different average intensity.

## ***Computational Models of Motor Adaptation***

Several groups have successfully constructed mathematical models that capture some of the key features of motor adaptation (Bays and Wolpert 2007; Bock 2003; Conditt et al. 1997; Conditt and Mussa-Ivaldi 1999; Fine and Thoroughman 2007; Kording et al. 2007; Korenberg and Ghahramani 2002; Lai et al. 2003; Scheidt et al. 2005; Scheidt et al. 2001; Scheidt et al. 2000; Scheidt and Stoeckmann 2007; Thoroughman and Shadmehr 2000). The typical observation is that the process is reasonably well described by a linear, constant-weighted sum of perturbation strengths (or load magnitudes) and kinematic errors from a limited memory of past attempts at the reaching task. The autoregressive, limited-memory model (8) proposed by Scheidt et al (2001) captures the relationship in a succinct manner and has been chosen to characterize motor adaptation in this experiment.

$$\boldsymbol{\varepsilon}_i = a_1 \boldsymbol{\varepsilon}_{i-1} + b_0 K_i + b_1 K_{i-1} \quad (8)$$

In this model,  $K_i$  and  $\boldsymbol{\varepsilon}_i$  are the magnitude of the stiffness load experienced in and the kinematic error resulting from the reach attempt for the upcoming trial  $i$ , respectively. Terms with an  $i-1$  subscript denote information experienced in the trial previous to trial  $i$ . This model uses both of the previous experience ( $\boldsymbol{\varepsilon}_{i-1}$ ,  $K_{i-1}$ ) terms and the load magnitude in the upcoming trial ( $K_i$ ) to predict performance ( $\boldsymbol{\varepsilon}_i$ ) in the upcoming trial. Model coefficient  $b_0$  characterizes the relationship between the load stiffness and kinematic error in the upcoming trial lending to an interpretation as the “effective endpoint compliance” of the adapting motor system. Model coefficient  $b_1$  describes the relationship of the previously experienced load stiffness to the error in the upcoming trial indicating the degree of influence this past experience had on the motor planning for the upcoming trial; this term will be described as the “influence of prior load.” The final model coefficient  $a_1$  relates the kinematic error on

the previous trial to that on the upcoming trial. This term will be interpreted as the “influence of previous error” on the upcoming motor plan. The model can also be rewritten in transfer function notation (9) using the  $z$ -transform and interpreted as a filter that transforms load stiffness information into kinematic error. In this form,  $a_1$  is the system pole, which specifies the decay rate of the system output. This transfer function representation also defines a system zero of  $-b_1/b_0$ , which reflects a compromise between transient response fidelity and steady-state response accuracy.

$$H(z) = \frac{E(z)}{B(z)} = \frac{b_0 + b_1 z^{-1}}{1 - a_1 z^{-1}} = b_0 \frac{1 + b_1/b_0 z^{-1}}{1 - a_1 z^{-1}} \quad (9)$$

Recent experimental evidence suggests that motor adaptation is not a fixed process, but rather that adaptation itself changes depending on environmental context. For example, Fine and Thoroughman (2006, 2007) looked at the adaptive response of reaching movements to brief environmental disturbances that varied in their time of onset within a movement as well as in their relative frequency across movements. In the first study, subjects were perturbed by brief force pulses that occurred pseudo-randomly at one of several distances along the reach path and with pseudo-random direction (leftward or rightward) and in one experiment the force pulse also had a pseudo-randomly selected amplitude from the set {6, 12, 18} N. Force pulses were experienced in 20% of the experienced reaching trials and were never experienced consecutively. Adaptation was quantified by the difference in perpendicular deviation of the hand path between the post-pulse and pre-pulse trial. From this they observed only a categorical adaptation; on average subjects only demonstrated a direction-dependent response to the perturbations, even those that varied in magnitude. In the second study, subjects’ reaches were perturbed in 80% of trials by a viscous-curl field with strength that varied pseudo-randomly according to one of three distributions (each

distribution contained 6 field strengths). The distributions were described as strongly-biased, weakly-biased, and zero-biased. The strongly-biased distribution contained only field strengths that were directed either leftward or rightward depending on the subject group. The weakly biased distribution contained four field strengths directed in the same subject-group-dependent direction and two in the opposite direction. Finally, the zero-biased distribution contained equal number of leftward and rightward directed field strengths. Using these perturbations, these researchers found that subjects expressed categorical adaptation for all but the strongly-biased distribution. They also found that reducing the proportion of perturbed trials for the strongly-biased distribution to 50% or 20% restored the categorical adaptive response. For this study, Fine and Thoroughman used a state-space model, which was of a form that was demonstrated to be algebraically equivalent to the model used in this work to analyze motor adaptation (Scheidt 2004; Scheidt et al. 2001). Despite observations of categorical adaptation, this proportional adaptation model was able to account for more than 98% of the variance in the behavioral data for all conditions. These observations support the broad utility of limited memory models of motor adaptation under a variety of experimental conditions.

## RESEARCH METHODS

Fourteen subjects (4 female; median age of 24 years; range: 18 to 58 years) provided informed consent to participate in these experiments. All experimental procedures were approved by Marquette University's Office of Research Compliance as Protocol # HR-1179.

Subjects were instructed to reach smoothly and accurately with their right hand out-and-back from a single home position to a fixed target position 10 *cm* anterior to the home (the goal) while holding the handle of a 2-DOF robotic manipulandum (i.e. a "reach-and-return" motion). A lightweight, low-friction arm trough supported the reaching arm against gravity throughout the experiment. The home and goal target locations were presented visually on all trials as 1 cm diameter circles projected on to a horizontal screen directly above the plane of arm motion. On some trials (described below), a cursor was also projected directly above the hand's location at the peak reach extent as a 5 mm diameter circle providing visual feedback (knowledge of results) of reach extent. The projection screen blocked direct view of the arm throughout the experimental session. Volunteers were instructed to make movements such that the centrifugal (outward) phase took  $250 \pm 13$  *ms* ( $\pm 5\%$ ) to execute. Feedback of movement time was provided visually using a linear scale that appeared at the end of each trial. The desired movement time of 250 *ms* was clearly indicated on the display, and the scale changed color depending on whether movement time was within (green), greater than (blue), or less than (red) the desired range. Thus, a blue time bar indicated that the movement was too slow and a red corresponded to a faster movement than desired.

## ***Data Collection***

The robotic manipulandum recorded the forces, moments, and linear and angular accelerations at the subject's hand using an analog 12-DOF load cell (Model 200N12, JR3, Woodland, CA) and the angular position of each motor shaft using 17-bit absolute encoders (Gurley Precision Instruments, Troy, NY). These data were acquired at 1 kHz by analog-to-digital (A/D) conversion (Model PCI 6031E, National Instruments, Austin, TX) and digital input/output (I/O) hardware (Model PCI DIO48H, Computer Boards, Norton, MA) for these two types of sensors, respectively. The analog signals from the 12-DOF load cell were low-pass, anti-alias filtered at 500 Hz prior to A/D conversion. These data were stored to hard disk as well as used to control the manipulandum throughout the experiment. In addition, the commanded motor torques, Cartesian position of the manipulandum handle, and the parameters of the trial configuration were recorded to hard disk for post processing and verification of manipulandum performance.

Bipolar, differential EMG electrodes (Model Bagnoli-8 system with Model DE2.1 electrodes, Delsys, Boston, MA) were attached to the skin over the muscle bellies of eight arm and shoulder muscles: brachioradialis (BRD), lateral head of the biceps brachii (BiLat), medial head of the biceps brachii (BiMed), long head of the triceps brachii (TriLong), lateral head of the triceps brachii (TriLat), pectoralis major (Pec), anterior deltoid (AD), and posterior deltoid (PD). EMG signals were band-pass filtered to a range of 20 to 450 Hz by the EMG hardware, prior to A/D conversion at 1000 Hz. Limb segment lengths were measured with a tape measure and joint angles were measured with a goniometer while the subject held the handle of the 2-DOF robot at both the home and goal target positions. The upper arm length was measured from the acromion (scapula) to the lateral epicondyle (humerus) and the lower arm length was measured from the lateral epicondyle (humerus) to

the center of the handle of the 2-DOF robotic manipulandum. The joint angles were measured with the arms of the goniometer centered on the limb segments and the goniometer hinge centered over the bony landmarks. Subjects' wrists were splinted in a neutral position during experimentation to allow the forearm and hand to be treated as a single link.

### ***Experimental Protocol***

During the experimental session, subjects performed six blocks of 151 reaching movements while the robot simulated mechanical loads consisting of a 2 kg point mass connected to one end of a spring-like load which was, in turn, connected on the other end to the home target location (Figure 1). The robot also constrained hand motion to the line perpendicular to the subject's chest (i.e. the y-axis of the robot's reference frame) using stiff PID position control. The environmental loads can be summarized by the following pair of equations:

$$\begin{aligned} F_x &= G_p d_x + G_I \int d_x + G_D \dot{d}_x \\ F_y &= m \ddot{d}_y + c \dot{d}_y + k d_y \end{aligned} \tag{10}$$

where  $F_x, F_y$  are the forces generated by the manipulandum;  $d_x, d_y, \dot{d}_x, \dot{d}_y, \ddot{d}_x, \ddot{d}_y$  are x- and y-axis components of hand displacement, velocity, and acceleration from the home target location, respectively;  $m, c, k$  are the mass, viscous friction, and stiffness properties on the system along the y-axis (anterior-posterior movement); and  $G_p, G_I, G_D$  are the gains of the stiff PID controller acting along the x-axis (lateral movement). The system viscosity in the direction of movement ( $c = 10 \text{ N s/m}$ ) was constant across all trials and was

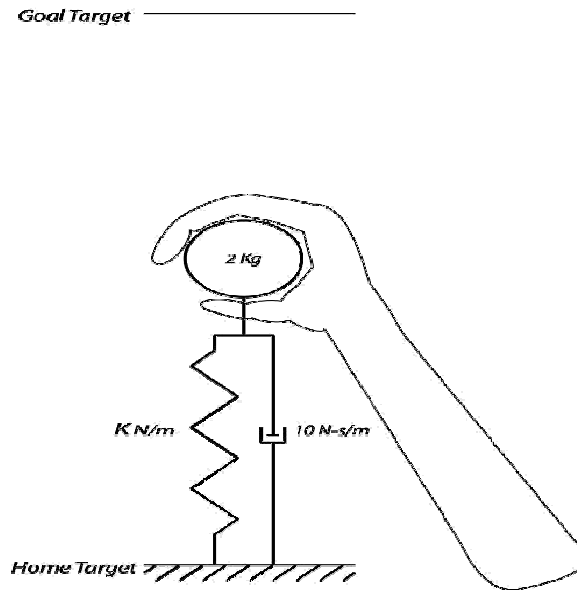


**Figure 1: Diagrammatic Representation of the Mechanical Environment**

included to promote stability of motion. Only the stiffness of the virtual spring ( $k$ ) changed during the experimental sessions; changes in load stiffness were considered as perturbations which subjects must compensate in order to reach accurately from the home to goal targets. Manipulating the elastic component of the load resulted in a low average damping ratio ( $0.156 \pm 0.0140$ ) that demonstrated only minute variation. The natural frequency ( $17.2 \pm 1.4 \text{ Hz}$ ) remained well above the frequency content of the subjects reaches (approximately 0 to 2  $\text{Hz}$ ) and also did not vary greatly. The loads presented to subjects had consistent and stable behavior over the course of the experiment.

Prior to the experimental session, subjects were permitted to practice reaching against the load with a very weak elastic component ( $25 \text{ N/m}$ ) to allow for familiarization with the required task and timing. Once subjects became comfortable with the task, they were guided through two sets of maximum voluntary contraction (MVC) exercises while the researcher provided the resistance. Each set of MVC exercises consisted of a maximal contraction in elbow flexion, elbow extension, shoulder horizontal abduction, and shoulder

horizontal adduction while the arm was held in the approximate configuration attained during experimentation. After a short break, an initial *Effort-Test* trial was performed against a stiff load of 1000  $N/m$  to establish a baseline set of EMG activity for later comparison. During *Effort-Test* trials, subjects were asked to reach to the target and hold it there for five seconds before bringing their hand back to the home position. Concurrent cursor feedback of hand position was provided in this phase to facilitate target acquisition and maintenance. In all other trials, subjects were asked to reach-and-return in one fluid movement (i.e. with no pause at the distal target).

Each block of trials was comprised of five separate phases, and the six trial blocks differed in the mean and variability of the spring-like loads applied during the fourth (test) phase. Each block started with 20 trials (phase 1; practice) in which subject practiced moving against the average load they would experience in the upcoming test phase. In these trials, visual feedback of maximum reach extent (a cursor projected directly above the farthest hand position from the home target location) was provided so that subjects could calibrate their reach extent for the upcoming test phase. The next 5 trials (phase 2; baseline) were also performed against the average load to be experienced in the upcoming test phase, but here visual feedback of reach extent was eliminated. The purpose of these trials was to provide an estimate the subject's average performance while reaching against the current mean load value to the remembered goal location without cursor feedback.

The next 100 trials (phase 3; test) were performed without visual feedback and against a sequence of spring-like loads that varied in magnitude from trial-to-trial. The stiffness values for each trial were predetermined and pseudo-random so each subject experienced the same sequence of loads for any given block. The descriptive statistics (mean and standard deviation) of the pseudo-random sequence for each block are described in

Table 1 and as histograms in Figure 2. All subjects experienced each of the six blocks over the course of the experimental session, and the presentation of blocks was randomized across subjects to minimize the effect of presentation order.

**Table 1: Experimental Condition Notation**

	Mean ( $N/m$ )			
	Low: 250	Mid: 500	High: 1000	
2 Standard Deviations ( $N/m$ )	Low: 80	mLvL	mMvL	mHvL
	Mid: 160		mMvM	
	High: 320		mMvH	mHvH

**Control Load Types: fixed stiffness**

*Constant:* very low stiffness ( $25 N/m$ ) for washout blocks.

*Effort-Test:* high stiffness ( $1000 N/m$ ) used for periodic fatigue monitoring.

**Experimental Load Types: pseudo-random, normally distributed stiffness (mean  $\pm$  2 standard deviations)**

**mLvL:** low mean, low variability set ( $250 \pm 80 N/m$ )

**mMvL:** middle mean, low variability set ( $500 \pm 80 N/m$ )

**mMvM:** middle mean, middle variability set ( $500 \pm 160 N/m$ )

**mMvH:** middle mean, high variability set ( $500 \pm 320 N/m$ )

**mHvL:** high mean, low variability set ( $1000 \pm 80 N/m$ )

**mHvH:** high mean, high variability set ( $1000 \pm 320 N/m$ )

**Load Contrast Levels:**

	Low	Mid	High
MEAN Contrast:	mLvL	mMvL	mHvL
VAR Contrast:	mMvL	mMvM	mMvH
WEBER Contrast:	mLvL	mMvM	mHvH

The next 25 trials (phase 4; washout) were performed against a load having a very weak elastic component ( $25 \text{ N/m}$ ). These trials required subjects to adapt to a very different load than they had just experienced, with the intention of minimizing carry-over of learning from one block of trials to the next. Previous work suggests that our 25-trial washout phase was sufficiently long regardless of potential differences in the adaptation to the washout phase load (Lai et al. 2003; Patton and Mussa-Ivaldi 2004; Scheidt et al. 2001).

The final reaching trial (phase 5; effort test) was performed in the same manner as the initial effort test preceding the experimental blocks. Including this trial in each block allowed us to calculate an EMG to force ratio (Kirsch and Rymer 1987) to assess the evolution of muscular fatigue throughout the experimental session. Each block was followed by a minimum of 2 minutes of rest that was intended to delay and reduce the onset of muscular fatigue.

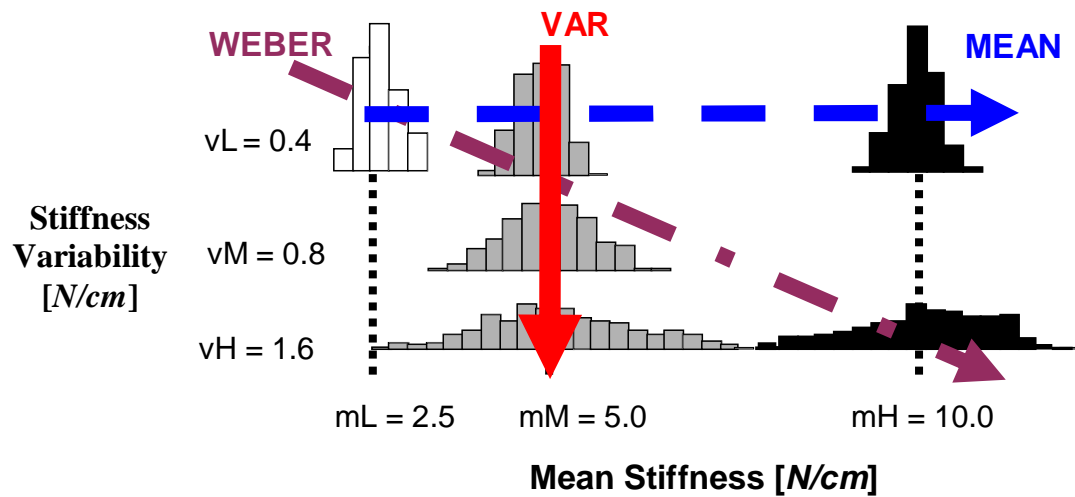


**Figure 2:** Histograms of stiffness distributions for experimental blocks.

The trial blocks were classified according to the mean ( $m$ ) and variability ( $v$ ) of the loads experienced during the experimental test phases: [ $mLvL$ ,  $mMvM$ ,  $mHvH$ ,  $mMvL$ ,  $mHvL$ ,  $mMvH$ ] depending on whether the mean or variability were defined to be low (L), middle

(M), or high (H) (Table 1). Each block was limited to a range equal to the specified mean  $\pm$  twice the specified standard deviation (variability). The sequences were designed so that they had no significant autocorrelation values beyond lag 0, by comparison to a 95% confidence interval (Figure 3). The six load types allowed motor adaptation to be modeled for three blocks each along three trends in load statistics that we will call contrasts. These contrasts are (1) increasing mean with constant standard deviation (MEAN contrast), (2) constant mean with increasing standard deviation (VAR contrast), and (3) equally increasing mean and standard deviation (WEBER contrast). Diagrammatically, these contrasts are shown by the arrows overlaid on the histograms presented in Figure 2. The experimental design used these six blocks – arranged as three contrasts – instead of all nine blocks representing each

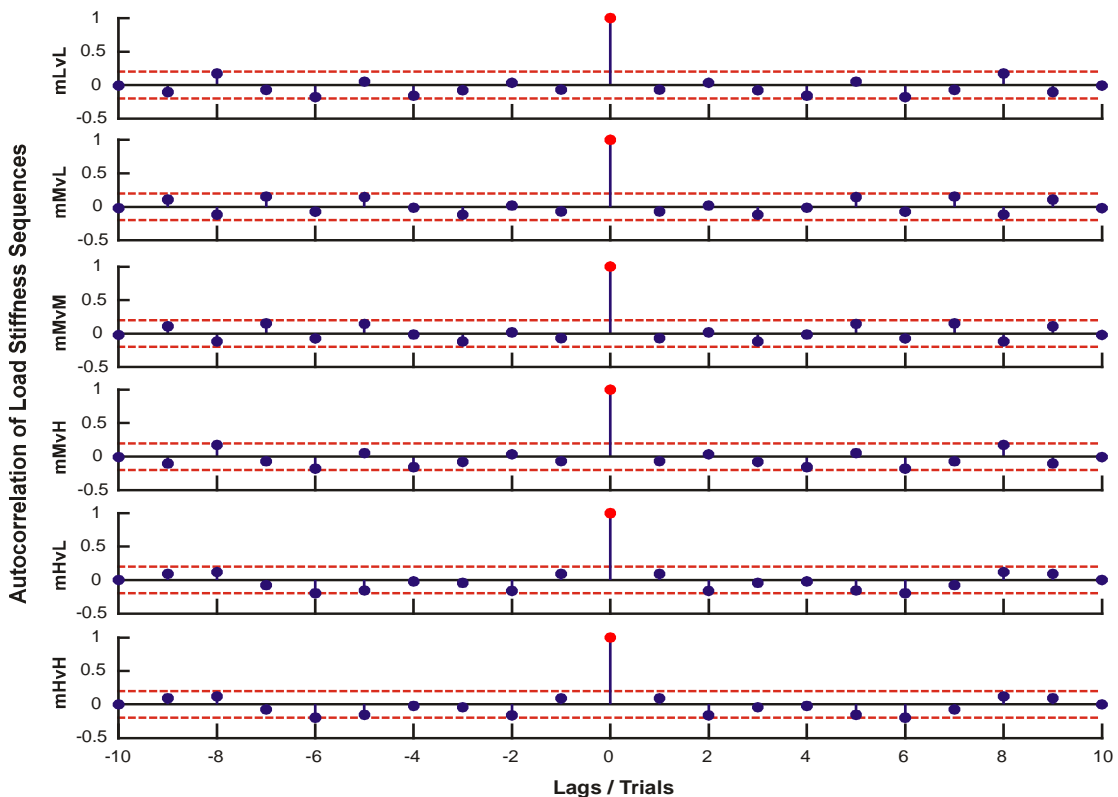


**Figure 3:** Autocorrelation values for the stiffness load series of each block of trials. Each block of stiffness loads only has a significant autocorrelation at lag 0. Red dashed lines represent the 95% confidence interval for  $H_0$ ; autocorrelation value at this lag is not different from 0.

combination of mean and standard deviation because we were concerned that the additional 375 trials would increase the risk of subject fatigue to an undesirable level.

### ***Data Analysis***

We evaluated whether there were systematic differences in the kinematics and kinetics of reaching as a function of block type using several performance measures. These included peak movement extent; peak velocity, acceleration, and force; and the reach extent at which these last three peak values occurred. All performance measures were obtained using an automated algorithm within the MATLAB computing environment (MathWorks, Natick, MA). Reach extent was taken as the furthest distance reached within a 200 *ms* window centered on the first time point where the outward reach velocity dropped below a threshold of 0.1 *m/s*. We then computed a scalar movement extent error ( $\varepsilon$ ) for each trial, which was the primary performance measure in subsequent analyses. Extent error was calculated as the signed difference between reach extent and the desired target distance of 10*cm*. The trial sequences of extent error  $\varepsilon$  and the load stiffness  $K$  were used to calculate weights in a motor learning model (8) developed by Scheidt and colleagues (Scheidt et al. 2001).

Before we used analyzed individual subject data, we wanted to assess whether these data demonstrate a similar relationship to that observed by Scheidt and colleagues (2001) and whether an alternate number of parameters would better describe the adaptive process under these experimental conditions. We used the MATLAB System Identification Toolbox to fit a set of higher-order models of the form (11), which the limited-memory, autoregressive models (8) in a member where  $L$  and  $M$  both equal 1 (have 1 history element). Since each

subject experienced the same pseudo-random stiffness load sequence for each block, we were able to average the extent errors made by subjects for each trial of each block, creating an ensemble average of extent error. This ensemble average of the extent error of all 14 subjects was used to calculate the coefficients of this set of models (11) for up to 10 trials into the past (L and M equal 10).

$$\mathcal{E}_i = \sum_{j=1}^{i-L} a_j \mathcal{E}_{i-j} + \sum_{k=0}^{i-M} b_k B_{i-k} \quad (11)$$

Ensemble averaging reduces the uncorrelated execution noise, which strengthens the underlying trend and allows the optimization algorithms to choose the best model more efficiently. In all cases, the linear trend was removed from the extent error and stiffness magnitude sets of each block to focus on the trial-to-trial relationships in the data. The block data were split in half; the last 50 trials were used to estimate the coefficients of the models for each block, and then the first 50 trials served to validate the respective models. Models were compared using the minimum descriptor length (MDL) criterion described by equation (12) (Ljung 1999), which determines the optimal model by minimizing a modified mean-squared-error (MSE) equation:

$$MSE_{MDL} = MSE \left( 1 + n \frac{\log(k)}{k} \right) \quad (12)$$

where  $n$  is the number of parameters in the model and  $k$  is the number of data points used to estimate the coefficients. This modification to the standard MSE equation balances model fit and complexity.

Once the appropriate model order had been determined, each subjects' reaching data was individually fit to the chosen model. The model coefficients were calculated using linear

regression methods in Minitab (MiniTab Inc., State College, PA). Linear trends were removed from each regressor (extent error and load stiffness) to focus regression on the trial-by-trial dynamics of the adaptation process. The regressors were transformed into principle components prior to regression analysis to provide a set of orthogonal signals that comply with the underlying assumptions of linear regression. The final coefficients were transformed back to "physical space" ( $\bar{q}_{phys}$ ) from "principle component space" ( $\bar{q}_{PC}$ ) using the correlation matrix ( $M_{corr}$ ) of the principle component analysis and the standard deviations of each regression signal ( $\bar{\sigma}_q$ ) calculated prior to the transformation (13).

$$\bar{q}_{phys} = (M_{corr} \bar{q}_{PC}) / \bar{\sigma}_q \quad (13)$$

Outlying data points were detected by inspecting externally Studentized residuals. Studentized residuals are equivalent to a t-statistic (Student's t-test) where the value of each residual is centered and scaled by the mean and standard deviation of the set of residuals. Externally Studentized residuals differ in that the mean and standard deviation used for each value comes from a separate run of the regression where the row of data corresponding to the particular residual has been removed. This process makes the externally Studentized residual more sensitive to situations where removing the row of data has a large impact on the statistics of the residuals. Comparing externally Studentized residuals against a threshold of  $\pm 3.75$ , represents a test for the presence of an outlier in a linear model with an  $\alpha$ -level of 0.01 as described by Lund (Lund 1975). We chose to use an  $\alpha$ -level of 0.01 to be very conservative on the removal of data because outlier removal was included only as a precaution. On average, one trial was removed from each subject's data as an outlier, which constitutes removal of approximately 0.167% of the data. The outlier with the largest

externally Studentized residual beyond the specified threshold was removed and the principle component analysis and linear regression described above were recomputed. Only one outlier was removed at a time to allow the principle components, regression coefficients, and externally Studentized residuals to be recalculated without the potentially misleading data point.

### ***Statistical Hypothesis Testing***

Extent error and movement time were compared to the target regions ( $\pm 0.5$  cm target region and  $250 \pm 13$  ms ( $\pm 5\%$ ) movement time, respectively) using one-sample t-tests against the bounds of these target regions (see Results). For our remaining kinematic and kinetic performance metrics, each peak measure, and the reach extent at which it occurred, was analyzed using ANOVA to look for systematic trends as a function of contrast level within each contrast separately. The three contrasts (MEAN, VAR, and WEBER) were analyzed using repeated measures ANOVA to detect trends in adaptation strategies, as predicted by the limited memory model of motor adaptation. Whenever a significant trend was found by ANOVA, *post hoc* t-tests were always conducted using the Tukey method. The one-sample t-tests and the ANOVA's (as well as subsequent Tukey *post hoc* t-tests) assumed an alpha level of 0.05. This analysis on model parameters was discussed with Dr. Bansal of the Marquette University Mathematics, Statistics, and Computer Science Department, who has determined that it appears reasonable.

## ***EMG Analysis***

Average EMG data as a function of contrast level was inspected to look for trends in bulk muscle activity in response to our experimental conditions. EMG signals were processed by removing the mean of the raw signal then rectifying and smoothing the signal. The data was smoothed using a moving-window-average filter with a 50 *ms* window. This filter smoothes the signal by computing the average over a window of data 50 *ms* long then the window is shifted over sample-by-sample and a new average is calculated at each point. Rectified, smoothed EMG signals were then processed in two ways. First, it was averaged across trials within each of the 6 experimental blocks to get an average time series for each block for each subject. Second, it was integrated over the duration of each trial to get a scalar EMG magnitude for each trial. These integrated EMG values were then averaged across the trials within each block for each subject. The average integrated EMG for each block and each subject were then inspected using one-way, repeated-measures ANOVA for each muscle separately. Significant trends found by ANOVA were further analyzed using Tukey *post hoc* tests.

## ***Fatigue Assessment***

In an effort to quantify the progression of fatigue of the course of the experiment, we analyzed the trends of a metric roughly adopted from Kirsch and Rymer (Kirsch and Rymer 1992; 1987). The fatigue metric consisted of the ratio of the average of the EMG (as %MVC) divided by the average of the hand force measured while the subject applied a force against a 1000 N/*m* elastic load. The averages were calculated after the applied force had reached a steady state up to either the end of the trial or the point at which the applied force

dropped below 10% of the target force (100N). These EMG to Force ratios were then standardized as a percent difference from the first Effort-Test trial. Finally, one-way, repeated-measures ANOVA was used to determine whether there was a significant change in this ratio from the initial Effort-Test trial that might indicate that subjects experienced fatigue due to the loads.

## RESULTS

Subjects reached smoothly and accurately to the target in each training condition despite the frequent absence of concurrent visual feedback of hand trajectory (Figure 4). Reaches had a single velocity peak in both the outward (centripetal) and inward (centrifugal) phases of movement. Across subjects, movements in all load conditions averaged within  $\pm 0.01m$  (10%) of the desired extent and  $\pm 15 ms$  (6%) of the desired movement time. Average movement extents were within the target region for all trial blocks ( $p > 0.175$  in all cases), with the grand average extent error for the entire protocol equal to  $-0.0004 \pm 0.0067 m$ . Average movement time was also within the specified range for each block ( $p \geq 0.12$  in all cases), with the grand average for the entire protocol equal to  $255 \pm 9 ms$ . Overall, subject performance complied with the both the positional and movement time requirements expressed to them during the instruction phase of this protocol.

ANOVA found that peak hand force varied significantly within the MEAN ( $F_{2,42} = 681.37, p < 0.00005$ ) and WEBER ( $F_{2,42} = 751.54, p < 0.00005$ ) contrasts, but not the VAR ( $F_{2,42} = 1.75, p = 0.191$ ) contrast. Within the MEAN and WEBER contrasts, all *post hoc* pairwise comparisons had a  $p$ -value less than 0.00005 by the Tukey method. Taken together, these three comparisons indicate more specifically that peak hand force (Figure 4) varied systematically with the prescribed mean of experimental blocks. Average peak forces by prescribed mean block stiffness were mLvX =  $10.8 \pm 1.50 N$ , mMvX =  $33.6 \pm 2.52 N$ , mHvX =  $73.2 \pm 4.04 N$ . These levels of average peak forces reflect the doubling of load stiffness with each increase in prescribed mean load.

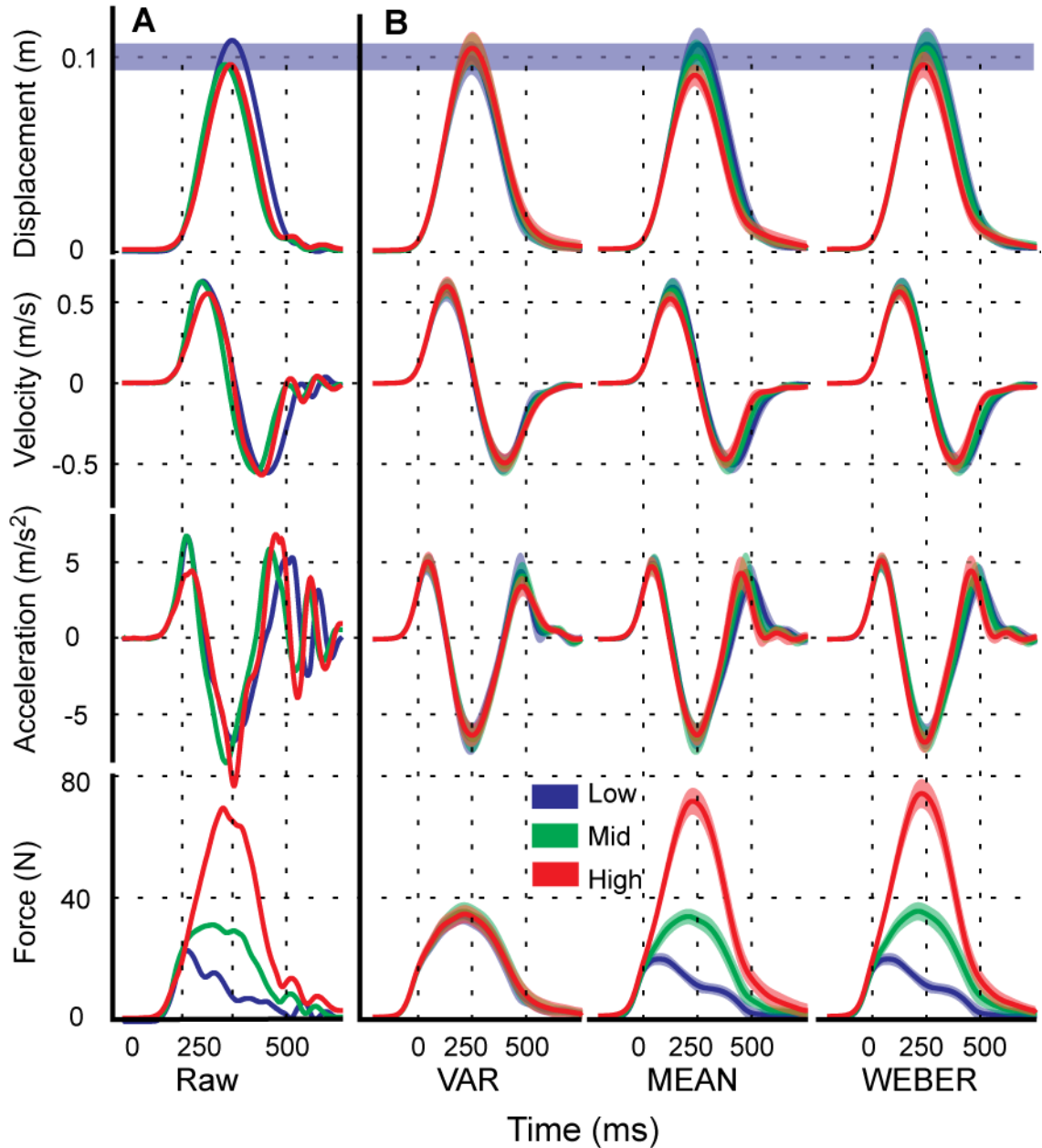


**Figure 4:** Kinematic and kinetic time series. The shaded region centered on 0.1 m for the displacement figures represents the size of the reach target. (A) Example raw data from a representative subject. One trial from each block of the MEAN contrast was included. (B) Average data across subjects by contrast level and grouped by contrast. Shaded regions around each trace represent  $\pm 2$  SEM from averaging across subjects.

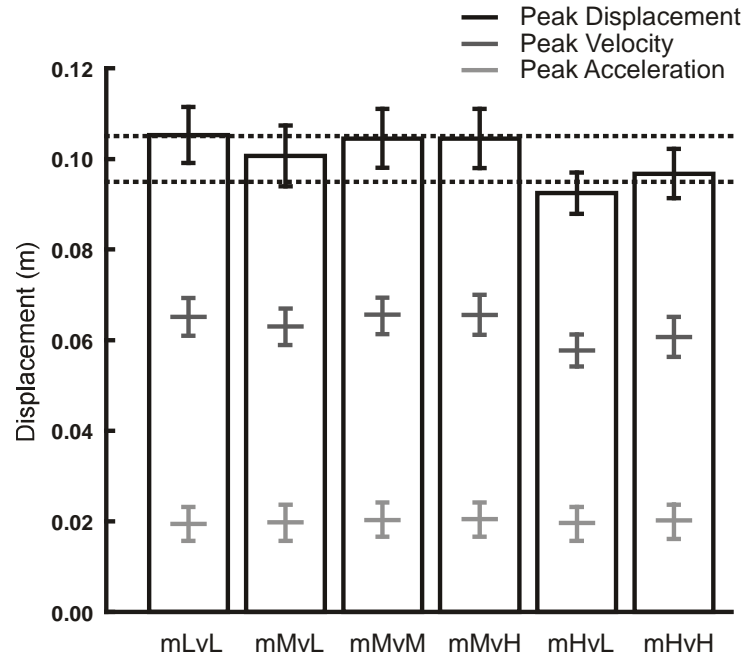


**Figure 5:** Average across subjects of peak displacement and displacement at peak velocity and peak acceleration by block. Error bars are  $\pm 2$  SEM.

### *Adaptation Model Structure Selection*

For each of the ensemble-averaged responses considered, movement errors elicited by interaction with the robot were reasonably well described as a linear function of load magnitude (Figure 6). We therefore used linear systems analysis techniques to characterize how subjects use information from prior reach-attempts to guide motor adaptation. Of all candidate models of moderate complexity having the form (11), the model (8) was identified as the minimum descriptor length (MDL) structure of choice for each of the six average responses. The MDL criterion indicated that the original model (8) described by Scheidt et al. (Scheidt et al. 2001) provided the most parsimonious representation of the adaptive process for all six blocks. Higher order models offered negligible improvement to model performance. The AIC algorithm typically chose models with an average of  $4.5 \pm 2.3$  additional parameters for stiffness and  $2.2 \pm 0.61$  more for extent error, these models only

demonstrated an average improvement of  $1.63 \pm 0.85 \%VAF$ . For a few blocks, the systems identification suite found models even larger than those chosen by the AIC algorithm to have the highest VAF, but these models also provided little improvement in model fit. Given the model with best VAF for each block, the average improvement in fit over the model described in (8) was  $1.89 \pm 0.97 \%VAF$  and required  $6.33 \pm 3.0$  additional parameters, which represents an average improvement of  $0.35 \pm 0.15 \%VAF/parameter$ . The model described by (8) accounts for  $87.8 \pm 4.48 \%VAF$ , providing a parsimonious description of the data without incorporating extraneous terms. Thus, (8) captures the average trial-by-trial changes in movement error irrespective of load conditions.

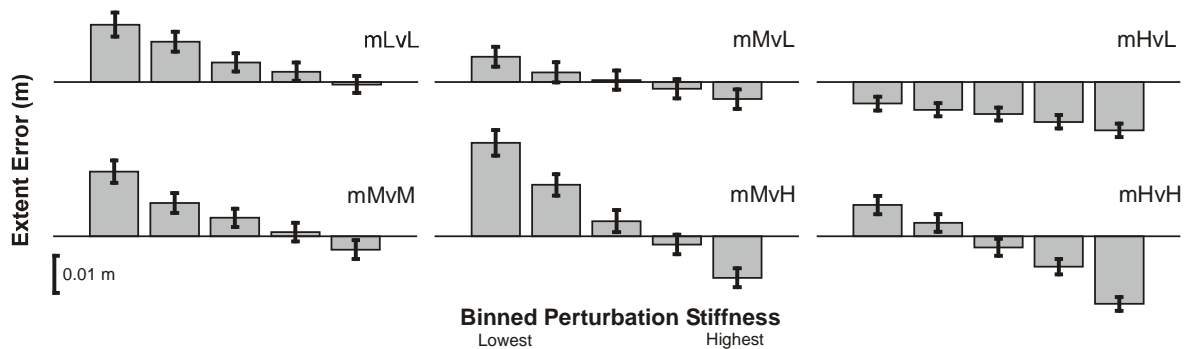


**Figure 6:** Average kinematic error by binned load stiffness values across subjects. Each bin represents 20% of the trials for the corresponding block where the trials have been sorted by the load stiffness from lowest (left) to highest (right). Plots illustrate the linear relationship between kinematic error and load stiffness. Error bars represent  $\pm 2$  SEM.

Adaptation models fit to individual subject data as described previously accounted for  $53.8\% \pm 4.20\%$  of the variance in their extent error. Of the three principle components used as regressors in each modeled data set (of which there were 14 subjects  $\times$  6 blocks = 84 modeled data sets), two or more of these principle components were significant ( $\alpha = 0.1$ ) regressors in 97.6% (82/84) of the modeled data sets. Every modeled data set had at least one significant principle component regressor after iterative removal of outlying data.

## ***Effect of Environmental Variability on Motor Command Updating***

The zero location in the adaptation model depended on the variability of the stiffness load sequence. Specifically, the VAR trend, which represented changes in load variability, demonstrated a decrease in the zero location as the variability of the blocks of environmental loads increased ( $F_{2,42} = 3.64, p = 0.040$ ). The zero location decreased an average of  $0.147 \pm 0.220$  per level of the contrast (Figure 7A), with a significant difference between the low and high variability conditions ( $p = 0.032$ ). Systematic changes were observed in the effective limb compliance ( $b_0$ ;  $F_{2,42} = 5.72, p = 0.009$ ) and in the influence of prior load ( $b_1$ ;  $F_{2,42} = 8.49, p = 0.001$ ) with increasing variability (Figure 7B). The influence of prior load decreased an average of  $0.212 \pm 0.206$  per contrast level with a significant difference between the low and high variance levels ( $p = 0.001$ ). Conversely, the effective limb compliance decreased  $0.103 \pm 0.122$  per level with increasing load variability, with a significant difference between the low and high variability levels ( $p = 0.006$ ).

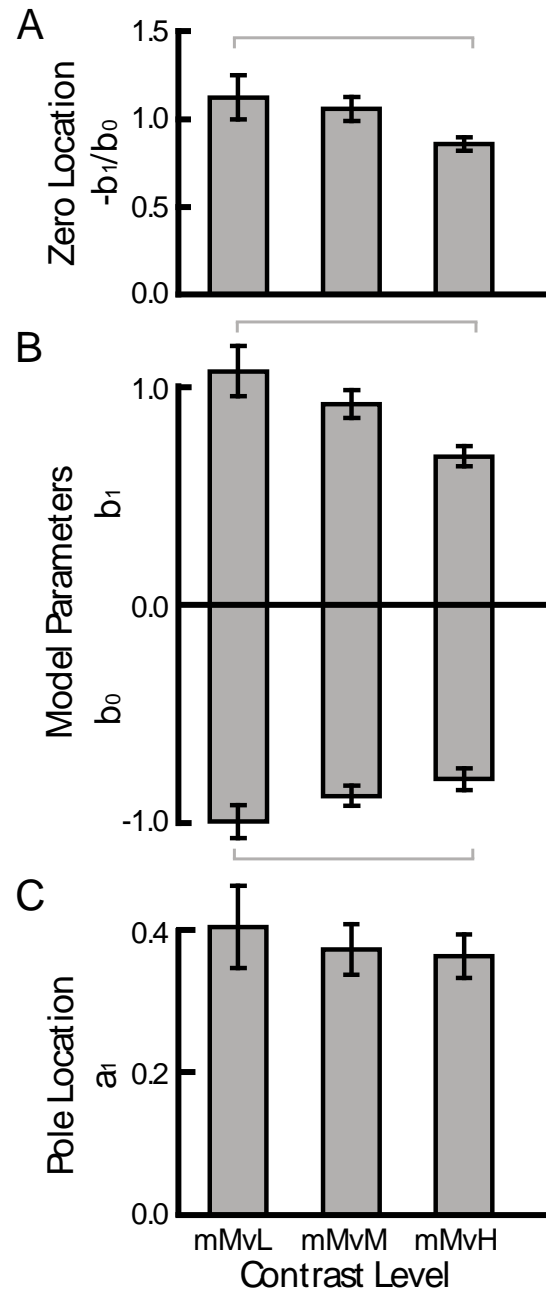


**Figure 7: Average adaptation model parameters for the VAR contrast (increasing load variability) across subjects. Error bars are  $\pm 2$  SEM and overbars indicate a statistically significant difference at  $\alpha = 0.05$ .**

Parameter  $a_i$  in the adaptation model (i.e. the transfer function pole location) did not change as the variability of the load sequence increased ( $VAR: F_{2,42} = 0.77, p = 0.474$ ). Average pole location was  $0.378 \pm 0.097$  for the VAR contrast (Figure 7C). Thus, changes to the impulse response of motor adaptation across training conditions in the VAR contrast were isolated to changes in the zero location of the transfer function. Specifically, the relative influence of prior load on motor adaptation decreased as environmental variability increased, and did so to a greater degree than the decrease in effective limb compliance, giving rise to this significant change in impulse response.

The observed trends were not a result of differences in movement extent. Across the VAR contrast, extent error was consistent ( $F_{2,42} = 2.01, p = 0.152$ ) averaging  $0.0031 \pm 0.0045 m$  (Figure 4). Peak velocity ( $0.589 \pm 0.0329 m/s$ ) and peak acceleration ( $5.15 \pm 0.320 m/s^2$ ) did not vary with contrast level within the VAR contrast ( $V_{MAX}: F_{2,42} = 0.84, p = 0.441$ ;  $A_{MAX}: F_{2,42} = 0.41, p = 0.670$ ). In addition, reach extent at peak velocity ( $0.0645 \pm 0.00328 m$ ) and reach extent at peak acceleration ( $0.0199 \pm 0.00178 m$ ) were consistent across the contrast (Figure 5:  $F_{2,42} = 1.75, p = 0.192$ ; Figure 5:  $F_{2,42} = 0.44, p = 0.649$ ). Consequently, trends in the model parameters for the VAR contrast are the result of the change in load variance rather than the result of differences in kinematic states visited along the trajectory.

### ***Effect of Mean Environmental Load on Motor Command Updating***

ANOVA found zero location to be consistent in the face of increasing mean load strength (Figure 8A:  $F_{2,42} = 1.47, p = 0.248$ ). This consistency was the result of strong opposing systematic variations in the model parameters values used to derive the zero location ( $b_0: F_{2,42} = 13.41, p < 0.0005$ ;  $b_i: F_{2,42} = 20.23, p < 0.0005$ ). Effective limb

compliance ( $b_0$ ) decreased  $0.341 \pm 0.263$  per level, while the influence of previous load ( $b_1$ ) decreased  $0.495 \pm 0.332$  per level (Figure 8B). So, even though the effective limb compliance decreased with increasing mean environmental stiffness, this was offset by a corresponding change in the influence of previous load in influencing upcoming motor commands. Thus, subjects maintained a similar transfer function zero location despite increases in mean stiffness.

In addition to the zero location, parameter  $a_1$  in the adaptation model (the transfer function pole location) also did not change significantly with the mean stiffness of the load sequence ( $F_{2,42} = 0.91, p = 0.417$ ), despite a four-fold increase in mean load stiffness. Average pole location was  $0.409 \pm 0.230$  for the MEAN contrast (Figure 8C).

Thus, the impulse response of motor adaptation did not vary significantly with

increasing mean load for the MEAN contrast despite decreases in effective limb compliance because it was balanced by a decrease in the influence of prior load.

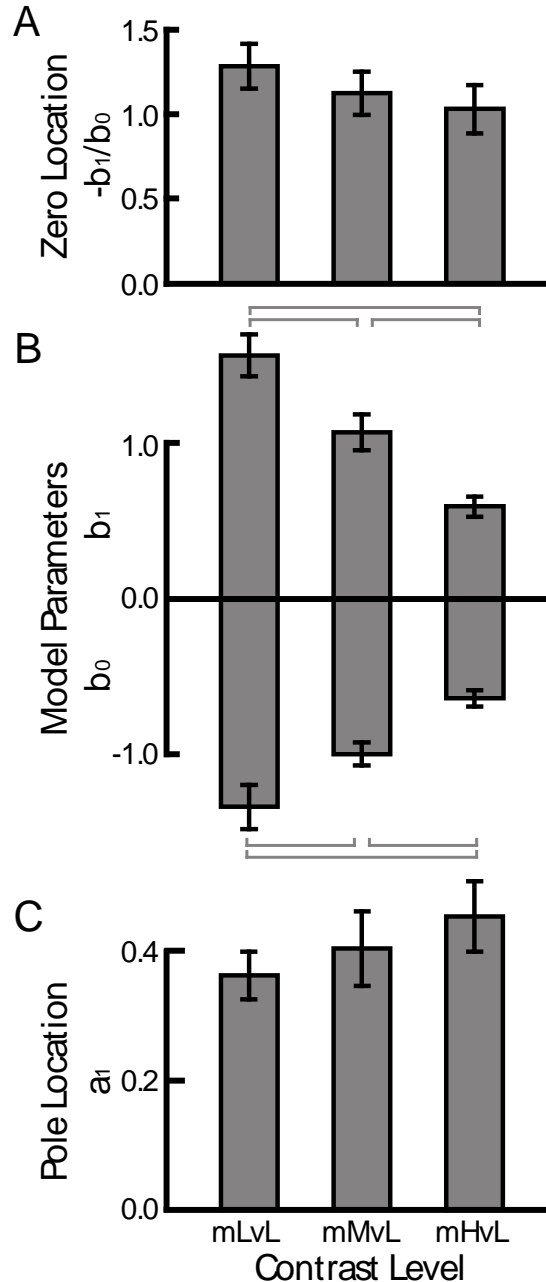


**Figure 8:** Average adaptation model parameters for the MEAN (increasing mean load) contrast across subjects. Error bars are  $\pm 2$  SEM and overbars indicate a statistically significant difference at  $\alpha = 0.05$ .

Although some differences in kinematics existed across the MEAN contrast, the trends in model parameters observed were due to increasing mean load rather than these differences. Extent error was significantly lower for the High level relative to the Low level for the MEAN contrast ( $F_{2,42} = 7.50, p = 0.002$ ), resulting in an average difference of  $0.0149 \pm 0.0042 \text{ m}$  ( $p = 0.0018$ ). The remaining pairs were not different from one another ( $p > 0.073$ ). While these values are significantly different, including extent error as a covariate had no observable effect on the significance of model parameters in the MEAN contrast (*i.e.*  $p < 0.01$  for  $b_0$  and  $b_i$ ). Extent error did not reach significance as a covariate for model parameters  $a_i$ ,  $b_i$ , and zero ( $p > 0.12$ ), but it did reach significance for  $b_0$  ( $p = 0.003$ ). Peak velocity was consistent ( $0.571 \pm 0.00191 \text{ m/s}$ ) as a function of contrast level ( $F_{2,42} = 2.48, p = 0.101$ ) in the MEAN contrast. Although peak velocity was consistent, differences in reach extent at peak velocity did vary with mean load strength (Figure 5:  $F_{2,42} = 6.92, p = 0.003$ ). Tukey *post hoc* testing revealed that reach extent at peak velocity for the High level ( $0.0563 \pm 0.00048 \text{ m}$ ) was significantly shorter (12.7%) than the other two levels of the contrast (Low:  $0.0660 \pm 0.00067 \text{ m}$ , Mid:  $0.0631 \pm 0.00074 \text{ m}$ ), which did not differ from each other ( $p = 0.544$ ). Reach extent at peak velocity did not reach significance as a covariate for model parameters  $a_i$ ,  $b_i$ , and zero ( $p > 0.20$ ), but it did reach significance for  $b_0$  ( $p = 0.012$ ). However, including reach extent at peak velocity as a covariate did not alter the significance of the model parameters for the MEAN contrast (*i.e.*  $p < 0.01$  for  $b_0$  and  $b_i$ ). Finally, peak acceleration (Figure 4:  $5.07 \pm 0.0413 \text{ m/s}^2$ ) and reach extent at peak acceleration (Figure 5:  $0.0193 \pm 0.00022 \text{ cm}$ ) did not vary across the MEAN contrast ( $F_{2,42} = 0.14, p = 0.871$  and  $F_{2,42} = 0.74, p = 0.486$ ). Taken together, these results demonstrate that the trends in model parameters observed in the MEAN contrast are a function of increasing mean load strength rather than the result of differences in peak kinematic states visited along the trajectory.

## Effect of ‘Weber-Equivalent’ Load on Motor Command Updating

The transfer function zero location was found to vary as a function of the simultaneous scaling of mean and variability in the WEBER contrast ( $F_{2,42} = 6.07, p = 0.007$ ). The average decrease in zero location was  $0.251 \pm 0.288$  per WEBER contrast level (Figure 9A) and paired *post hoc* Tukey tests indicated a significant decrease in zero location between the Low and High levels ( $p = 0.005$ ). This trend was the result of strong opposing (but unbalanced) systematic variations in model parameters used to derive the zero location ( $b_0$ :  $F_{2,42} = 26.44, p < 0.0005$ ;  $b_1$ :  $F_{2,42} = 40.58, p < 0.0005$ ). Effective limb compliance ( $b_0$ ) decreased  $0.372 \pm 0.206$  per level, while the influence of previous load ( $b_1$ ) decreased  $0.558 \pm 0.248$  per level (Figure 9B). So, even though the effective limb compliance decreased with increasing mean environmental stiffness, this was not fully offset by a corresponding decrease in the influence of previous load on upcoming motor commands resulting in a change in the impulse response of motor adaptation.

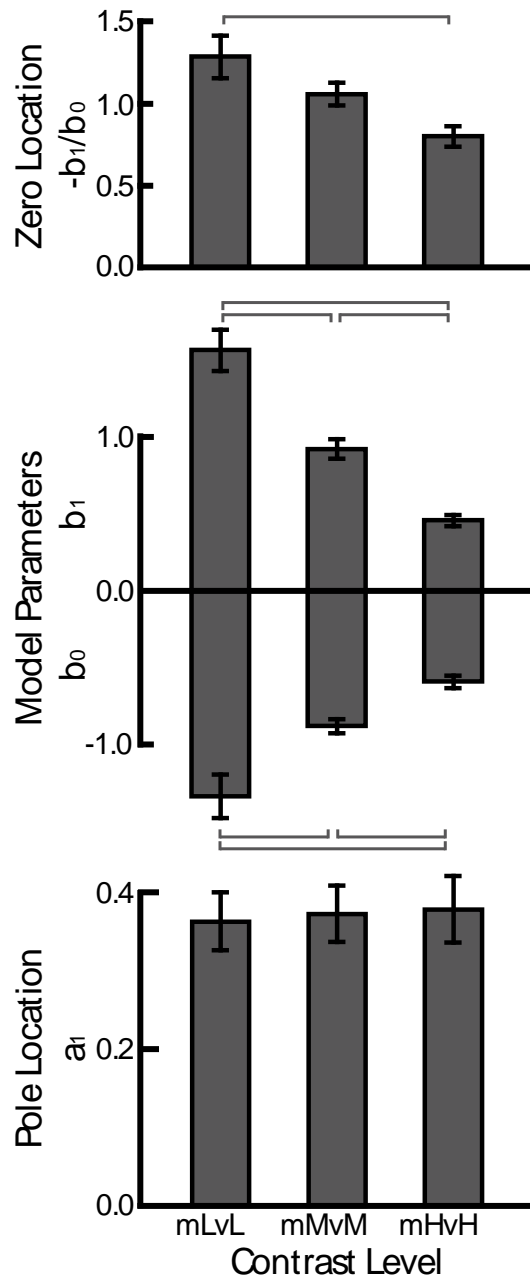


**Figure 9:** Average adaptation model parameters for the WEBER (simultaneously increasing load mean and variance) contrast across subjects. Error bars are  $\pm 2$  SEM and overbars indicate a statistically significant difference at  $\alpha = 0.05$ .

In contrast, parameter  $a_1$  in the adaptation model (*i.e.* the transfer function pole location) did not change with simultaneous scaling of mean stiffness and variability ( $F_{2,42} = 0.02, p = 0.985$ ). Average pole location was  $0.365 \pm 0.172$  for the WEBER contrast (Figure 9C). Thus, changes to the impulse response of motor adaptation across training conditions in the WEBER contrast were isolated to changes in the zero location of the transfer function (and specifically, to the mismatch between changes in the relative influence of prior load and changes in the effective limb compliance).

Extent error was significantly lower for the High level relative to the other two levels for the WEBER contrast ( $F_{2,42} = 8.59, p = 0.001$ ), resulting in an average difference of  $0.0099 \pm 0.0080$  *m* between the High level and the remaining two levels, which were not different from one another ( $p = 0.944$ ). While these values were significantly different, our systems identification techniques remove the mean extent error prior to modeling, thereby focusing on the trial-to-trial dynamics of motor adaptation. Extent error did not reach significance as a covariate for model parameters  $a_1$ ,  $b_1$ , and zero ( $p > 0.10$ ), but it did reach significance for  $b_0$  ( $p = 0.011$ ). However, including extent error as a covariate had no observable effect on the model parameter trends in the WEBER contrast ( $p < 0.04$  for  $b_0$ ,  $b_1$ , and zero). Peak velocity ( $0.591 \pm 0.0279$  *m/s*) and peak acceleration ( $5.29 \pm 0.268$  *m/s*<sup>2</sup>) did not vary with level in the WEBER contrast (Figure 5:  $V_{\text{MAX}}$ :  $F_{2,42} = 0.50, p = 0.613$ ,  $A_{\text{MAX}}$ :  $F_{2,42} = 0.56, p = 0.575$ ). Although peak velocity was consistent, significant differences in reach extent existed at peak velocity in the WEBER contrast ( $F_{2,42} = 6.13, p = 0.006$ ). Tukey *Post hoc* tests revealed that reach extent at peak velocity was significantly shorter (9.75%) for the High level ( $0.0597 \pm 0.00446$  *m*) relative to the remaining levels ( $0.0662 \pm 0.00273$  *m*) of the contrast (Figure 5), which were not significantly different from one another ( $p = 0.985$ ). Reach extent at peak velocity did not reach significance as a covariate for model parameters

$a_1$ ,  $b_1$ , and zero ( $p \geq 0.10$ ), but it did reach significance for  $b_0$  ( $p = 0.009$ ). However, including reach extent at peak velocity as a covariate did not alter the significance of the model parameters for the WEBER contrast (*i.e.*  $p < 0.04$  for  $b_0$ ,  $b_1$ , and zero). Reach extent at peak acceleration ( $0.0196 \pm 0.00158 \text{ m}$ ) did not vary as a function of level (Figure 5;  $F_{2,42} = 0.38$ ,  $p = 0.690$ ). Taken together, these results demonstrate that the trends observed in the WEBER contrast were due to the simultaneous increase in mean load strength and load variability rather than a result of variations in average peak kinematic states visited in each case.

### ***Lateral Forces Against the Stiff Controller***

Subjects were constrained to a straight-line out-and-back reach by a stiff PID controller. In this section, we will look at the average forces subjects applied against this stiff controller as a function of contrast level. The panels of Figure 10 provide views of three stages of the data processing that went into this analysis. Figure 10A provides examples of raw lateral force data from a representative subject. The averaged time series of lateral forces taken across subjects is shown in Figure 10B and the average lateral forces over the duration of the trial that we performed our statistics on are shown in Figure 10C with overbars to indicate significant differences in *post hoc* tests.

Average lateral forces exhibited by subjects while reaching increased significantly with increasing contrast level for those contrasts that included an increasing mean load (MEAN and WEBER) and no significant trend with changes in load variability (VAR). Lateral forces showed a significant increase (Figure 10C:  $F_{3,38} = 5.37$ ,  $p = 0.011$ ) with increasing MEAN contrast level with a significant difference between the Low and High levels according to *post hoc* Tukey tests ( $p = 0.0082$ ). In the WEBER contrast, lateral forces

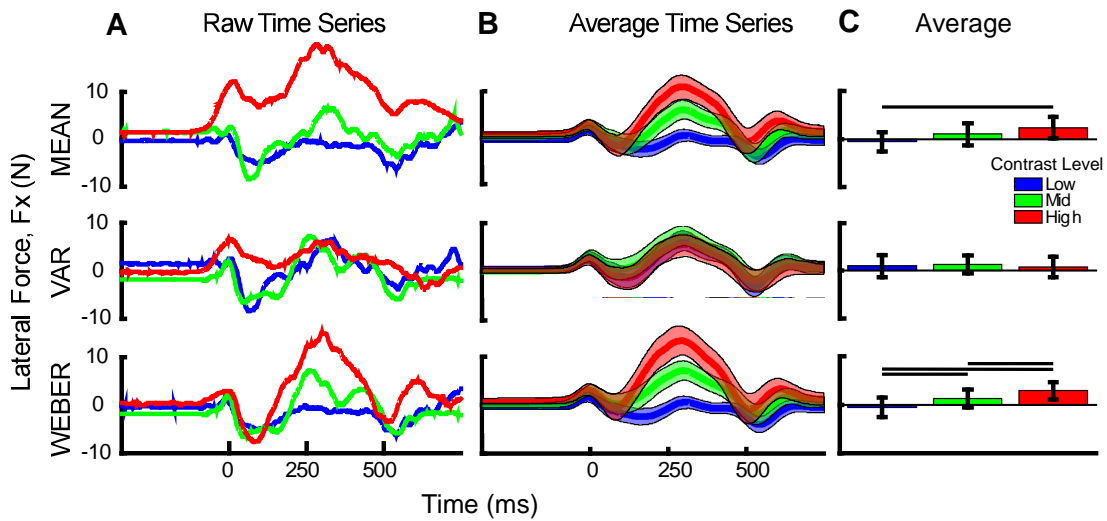


**Figure 10:** Lateral forces applied by subjects against the stiff controller. In each panel data is grouped by contrast (top: MEAN, center: VAR, bottom: WEBER) and contrast level (blue: Low, green: Mid, red: High) (A) Example force traces from a representative subject. (B) Average lateral force time series taken across subjects. Shaded region indicates  $\pm 2$  SEM from averaging across subjects. (C) Average lateral force taken over the duration of each trial. Error bars indicate  $\pm 2$  SEM from averaging across subjects and overbars denoted significant differences by Tukey *post hoc* test at  $\alpha = 0.05$ .

increased significantly with increasing contrast level (Figure 10C:  $F_{3,38} = 12.62, p < 0.0005$ ) with significant differences between the High level and both the Low and Mid levels ( $p \leq 0.026$ ). No significant trend in lateral forces was observed for the VAR contrast (Figure 10C:  $F_{3,38} = 0.38, p = 0.688$ ). Typically, these lateral forces were much smaller than the forces used to overcome the load (Figure 4). In all, lateral forces were small but increased significantly with increasing mean load and did not change significantly with changes in load variability.

### ***Effect of Multifactor Correlation on Model Fit***

The direct effect that load stiffness has on the kinematic error made in any given trial creates a correlation between the  $K_{i-1}$  and  $\varepsilon_{i-1}$  terms. Given that orthogonal predictors are an

underlying assumption of regression, it was necessary to verify that the contrast trends were not an artifact of violating this assumption. We used Principle Component Analysis (PCA) to create a set of orthogonal predictors to which our motor adaptation model was fit. The results of this analysis were similar to those of the previously mentioned analysis. In addition, we re-ran this PCA regression and set the coefficients that were not significantly different from zero ( $\alpha = 0.1$ ) to zero before transforming them back to load-stiffness-kinematic-error space (*i.e.*  $a_1, b_0, b_1$ ). This eliminated the effect of any uncorrelated PC's coefficient(s) on the final model parameters. The results of this PCA-regression method paralleled those of the previous PCA-regression method closely. We conducted an ANOVA in which we compared the model coefficients generated by these three regression methods. The results indicate that the regression method had no significant effect on model parameters overall (interaction: Method \* Parameter,  $F_{3,672} = 0.45, p = 0.715$ ) and had no significant effect on model parameters for each block (interaction: Method \* Parameter \* Block,  $F_{15,672} = 0.05, p = 1.000$ ), thus supporting the statistical inferences drawn for the results reported.

### ***Average EMG Trends by Contrast Level***

Average EMG signals for the primary agonists of this task scaled with the mean load stiffness for contrasts with changing mean load (MEAN and WEBER) and did not show a significant trend with load variability (VAR). One-way, repeated measures ANOVA were conducted across the levels of each block for each contrast and each muscle separately. Example rectified EMG signals from a representative subject are show in Figure 11A. Average EMG traces taken across subjects are depicted in Figure 11B with shaded regions

that indicate  $\pm 2$  SEM from averaging across subjects. These first two panels of Figure 11 provide a view of the intermediate stages of our data processing before moving on to the statistical analysis.

For the MEAN contrast, the agonists lateral head (TriLat; Figure 11C:  $F_{3,38} = 21.73$ ,  $p < 0.0005$ ) and long head (TriLong; Figure 11C:  $F_{3,38} = 17.15$ ,  $p < 0.0005$ ) of the triceps brachii showed significantly increased average activity with increasing mean load. Tukey *post hoc* tests for TriLat indicated significant differences existed between each contrast level with  $p \leq 0.026$  in each comparison. In post hoc tests, TriLong activity was significantly different at the High level as compared to the Low and Mid levels with  $p \leq 0.0044$  in both cases. The lateral head of the biceps brachii (an antagonist) also demonstrated a significant trend over the MEAN contrast (BiLat; Figure 11C:  $F_{3,38} = 4.46$ ,  $p = 0.023$ ) with one significant difference in post hoc testing between the Mid and High levels ( $p = 0.0312$ ). In the WEBER contrast, the agonists TriLat (Figure 11C:  $F_{3,38} = 22.31$ ,  $p < 0.0005$ ) and TriLong (Figure 11C:  $F_{3,38} = 12.74$ ,  $p < 0.0005$ ) as well as the anterior deltoid (AD; Figure 11C:  $F_{3,38} = 8.06$ ,  $p = 0.002$ ) also demonstrated significant scaling with load level. For all three muscles significant, along the WEBER contrast, differences existed between the High level and both the Low and Mid levels ( $p < 0.0208$  in all cases). Finally, there were no significant changes in EMG activity across all muscles measured for the VAR contrast (Figure 11C:  $F_{3,38} < 2.02$ ,  $p \geq 0.155$ ). In summary, agonist muscle EMG activity increased significantly with load level for both contrasts where we have increasing mean load (MEAN and WEBER) and did not change significantly when only load variability increased (VAR).

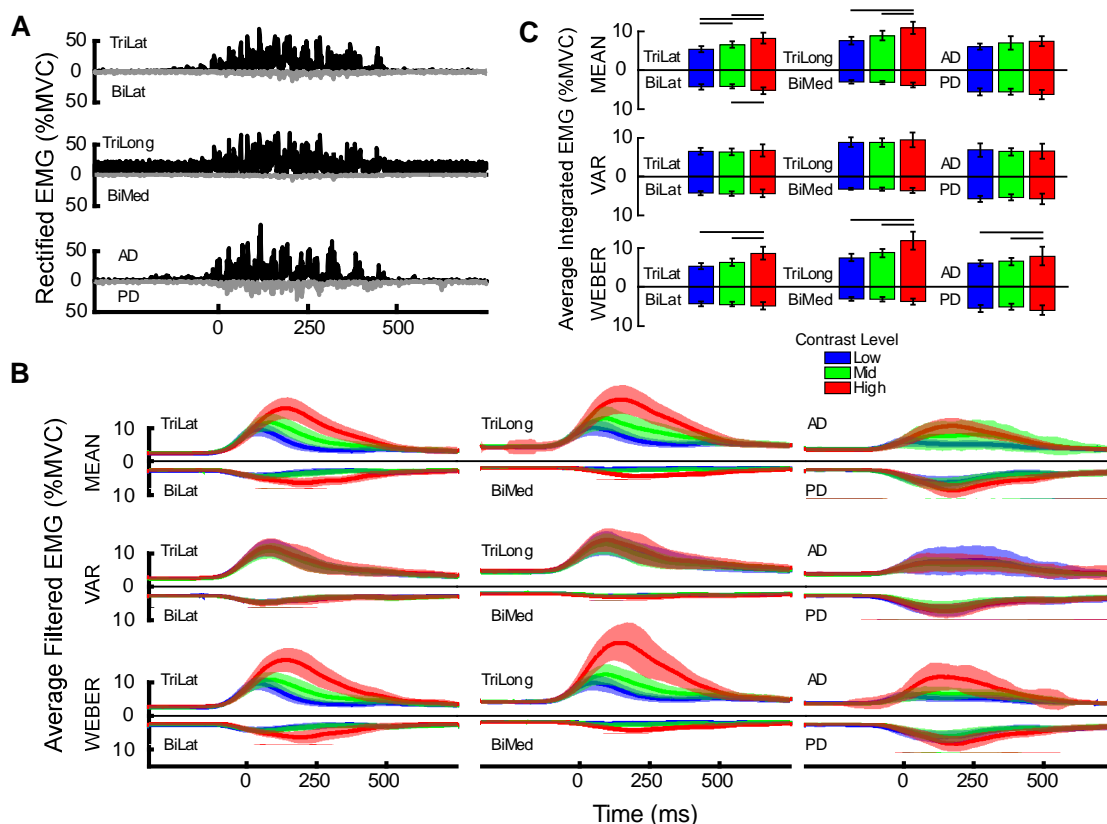


**Figure 11:** Raw and average EMG traces scaled as a percentage of MVC. In each panel, agonist muscles are plotted with increasing magnitude directed upward and antagonist are directed downward. (A) An example of rectified, raw EMG signals from a representative subject. (B) EMG time series averaged across subjects for each block of trials grouped by experimental contrast (MEAN, VAR, WEBER) and contrast level (Low, Mid, High). Shaded area surrounding the average EMG traces represents  $\pm 2$  SEM of the subject average. (C) Averages of EMG signals integrated over the duration of each trial. Error bars indicate  $\pm 2$  SEM of the subject average and overbars denote a statistically significant difference between contrast levels by Tukey post hoc tests at  $\alpha = 0.05$ .

## Fatigue

One-way, repeated-measures ANOVA indicated that no significant change (Figure 10:  $F_{6,96} < 1.32, p > 0.260$ ) in EMG to Force ratio from the initial “effort test” occurred across subjects in all muscles except the lateral triceps. While the lateral triceps did show a significant change in EMG to Force ratio (Figure 10:  $F_{6,96} = 2.75, p = 0.018$ ), the change was

an average decrease of  $11.3\% \pm 9.57\%$  relative to the value on the initial effort test ( $p < 0.04$ ). Although it did not reach significance, the average change in EMG to Force ratio was large ( $49.3\% \pm 65.9\%$  increase) for pectoralis on the 4 effort test. This is due to a single subject's measurement of a 378% increase for that trial. Without this one measurement, the average change in EMG to Force ratio was similar to the other trials ( $21.9\% \pm 41.0\%$ ). Note that Kirsch and Rymer found that EMG to Torque ratio nearly doubled as a result of fatigue and this effect lasted for at least 2 hours (Kirsch and Rymer 1987). This subject did not present this dramatic elevation in EMG to Force ratio in latter trials, which would have fallen into a 2 hour window, suggesting that this was not due to fatigue, but rather the effect of spurious performance error.

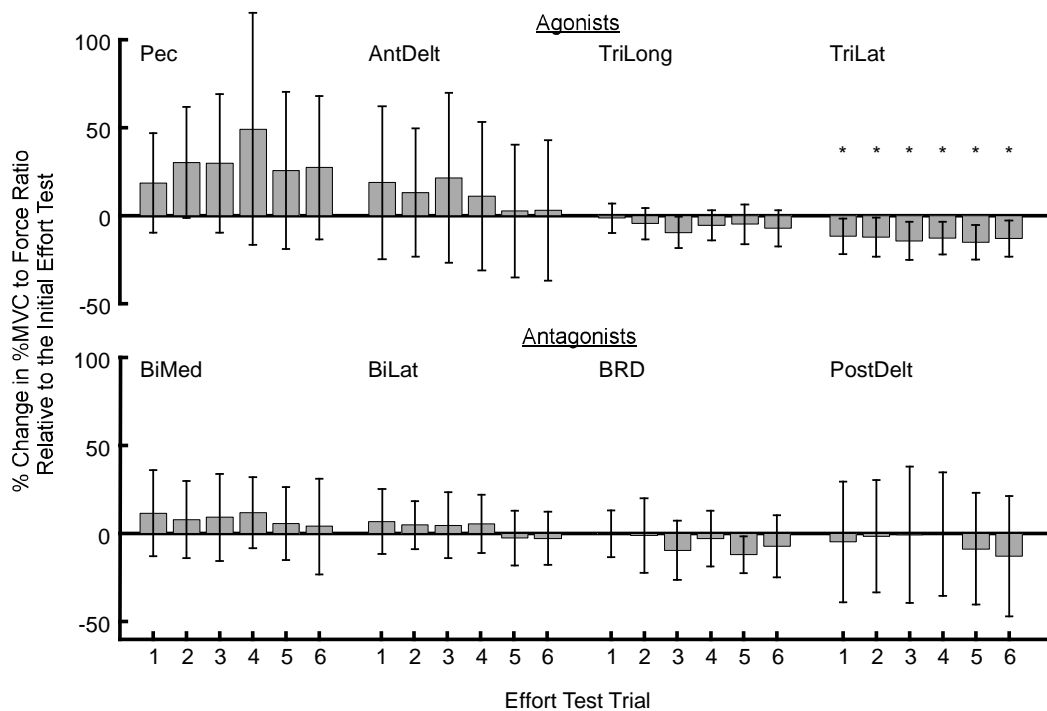


**Figure 12:** Average change in EMG to Force ratio for “effort test” trials relative to an initial “effort test” trial conducted prior to the first block of trials. Error bars indicate  $\pm 2$  SEM and \* indicates a statistically significant difference from the initial effort Tukey *post hoc* test at  $\alpha = 0.05$ .

## DISCUSSION

We sought to observe if and how sensorimotor information processing leading to motor adaptation may be sensitive to the statistical properties of the limb's mechanical environment. We explored this by requiring subjects to adapt a simple reaching task to 6 different blocks of environmental loads (each of which differed in mean and/or standard deviation of the load). We then identified the adaptation model structure and model coefficients for each block for subsequent comparison across training conditions. The model used (8) explained  $53.8\% \pm 4.20\%$  of the data variance in all six experimental conditions.

We found that, while  $b_0$  and  $b_1$  varied strongly with mean load (MEAN contrast), zero location varied with load variability (VAR contrast) rather than mean load. Specifically, ‘effective endpoint compliance’ ( $b_0$ ; also the system gain of the transfer function) strongly decreased and ‘influence of previous load’ ( $b_1$ ) strongly decreased with increasing mean load, but these trends presented to a smaller degree with load variability. Despite the strong trends, the zero location showed no significant relationship to changes in mean load stiffness, while it decreased with increasing variability. Recall that the strong trends in the  $b_0$  and  $b_1$  terms are not simply a result of numerically larger load stiffness terms since the mean value was removed prior to model fitting. From a transfer function perspective, the zero location controls the model responsiveness at the cost of steady-state error. The observed reduction in the zero location indicates a reduction in model responsiveness to past experience in response to increased uncertainty.

This trend of decreasing the influence of previous load in response to increasing load variability parallels a Bayesian model like the Kalman filter, described previously. Specifically, decreasing the influence of previous load on upcoming reaches is similar to changing the gain ( $K$ ) of the Kalman filter. From the equation for the Kalman filter gain (4), this behavior would indicate an increase in measurement uncertainty ( $\sigma_z^2$ ) rather than an increase in the predicted (prior) uncertainty of the environment ( $\sigma_i^{2-}$ ). This would imply that subjects are treating the random loads as noise injected into some “true environment” whose magnitude they are trying to estimate. This “true environment” would likely be the mean stiffness of the environmental load. If subjects were able to converge on an estimate of the mean environmental load and move to minimize end point errors assuming the mean environmental load, in our case of unautocorrelated loads, there should be no significant autocorrelation to the end point errors made. That assumes that the adapting individual maintains a long enough memory to determine the true mean and variance of the load for the entire block of trials, which is unlikely in our case of 100 trials. This would mean that a short term estimate must be used and the evolution of this estimate will have significant autocorrelation and will likely be similar to a random walk under our conditions. Movements made under the guidance of an estimate following this description could very well have given rise to end point error that are autocorrelated despite a lack of significant autocorrelation in the perturbing environment.

With this work, we have examined the response of motor adaptation to a range of load magnitude and variability combinations, we have demonstrated that the human motor adaptation is capable of tuning itself as appropriate for the level of noise it must contend with, and it does so in a manner that would be well described by Bayesian models.

### ***Zero Location Changes with the Variability of the Load***

There exists a strong relationship between changes in load variability and the relative influence of previous load. As environmental variability increases, there is rarely a period of steady-state input, and thus it seems appropriate for steady-state accuracy to decrease in behavioral importance. By sacrificing steady-state accuracy in favor of transient response fidelity, reaching end point error can be reduced. Conversely, when load variability is small and loads are consistent from trial-to-trial, end point error would be minimized by a strategy that emphasizes steady-state performance over transient behavior. Thus, the motor adaptation appears to be able to minimize reaching extent errors within a given environmental context, wherein the statistical properties of the load play a principal role in defining that context. Specifically, end point error is minimized by adjusting the balance between transient response fidelity and steady state accuracy on a trial-by-trial basis.

To clarify the tradeoff between steady-state and transient responses with changes in filter zero location, we have calculated the step and impulse response for a set of filters with evenly spaced zero locations (Figure 11). These filters had the same form as the motor adaptation model we used and were specified with unity (1) gain and a pole location at the origin (0) to focus on the effect of changing zero location. In our context, the input is load stiffness and the output of these filters is reaching error so an output value that approaches zero is ideal. As zero location approaches a value of 1.00, the output goes to zero after the initial change in the step load stiffness input (Figure 11A and 11C). However, a zero location of 1.00 will lead to an equal and oppositely directed error (*i.e.* transient error or aftereffect) on the trial following a single trial with a load (impulse), while smaller values for zero location will reduce this error in the transient response (Figure 11B and 11D). In this

way, a particular value of zero location will not be sufficient to reduce the reaching error for both a step and impulse inputs and the best choice will depend on the nature of the input.

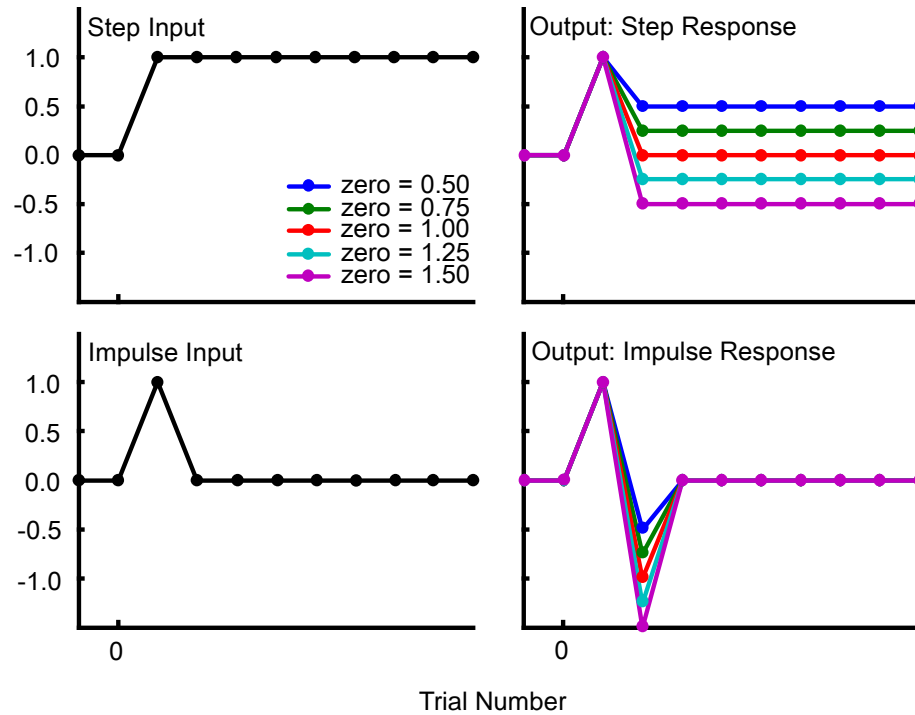


**Figure 13:** Step and impulse response plots for a selection of zero location values. These filter responses were calculated for filters with the same form used to model motor adaptation in this work. Unity gain and a pole located at the origin were used for each filter to isolate the effect of changing the zero location. (A) The step input to the filters. (B) The impulse input to the filters. (C) Step response for filters with evenly spaced zero locations demonstrating the change in steady-state error with increasing zero location. (D) Impulse response for the same filters as in C demonstrating the change in transient response with increasing zero location. Recall that the output is reaching error so 0 is the desired output.

### *Pole Location ( $a_1$ ) Does Not Vary With Load*

We did not find that subjects changed the relative contribution of prior kinematic errors on subsequent motor commands in response to systematic changes in the statistical properties of the environmental load. Muscle spindle sensitivity is known to depend on  $\gamma$ -fusimotor drive (Granit, 1970; Rothwell, 1994), which we expected to increase with

increasing average load magnitude. This led us to expect that system pole location  $a_1$  would have covaried with mean load strength. A strong effect confirming this prediction was not observed. Burge et al (2008) also observed invariance in the weighting of previous error in subjects reaching with random perturbations, while observing changes in response to random walks of varying standard deviations. The invariability we observed in weighting of previous error may be due to the lack of significant autocorrelation in our load sequences. When dealing with a load lacking significant auto-correlation, there would be little value in varying the weighting of previous error to the statistics of the load. While the weighting of previous error did not vary with the statistics of the perturbing loads, it was significantly different from zero. Since the value of  $a_1$  was positive in all cases and there was no significant autocorrelation in the load sequences, subjects made reaching errors that were correlated to the previous error (autocorrelated). If this parameter had been negative, subjects would alternate between ‘undershooting’ and ‘overshooting’ in the first few trials until they converged on an accurate motor plan (as was demonstrated previously in a simulation (Scheidt et al. 2001)). This oscillatory trend was not observed in much of the motor adaptation literature (Conditt et al. 1997; Kirsch and Rymer 1992; Scheidt et al. 2001; Scheidt and Stoeckmann 2007; Takahashi et al. 2006). Taken together, these observations may indicate that subjects cannot completely ignore reaching errors even when they are made against an uncorrelated trial-by-trial variation in load and would, consequently, provide less useful information for reducing reach end point error.

### ***The Role of Limb Compliance in Reach Accuracy***

Previous work has demonstrated that endpoint (or hand) compliance decreases in direct proportion to the kinetic demand required in overcoming a perturbing load during movement (Franklin et al. 2003) as well as posture maintenance (Franklin and Milner 2003; Gomi and Osu 1998; Perreault et al. 2004). We observed significant increases in agonist muscle activity with increasing mean load (kinetic demand) across the MEAN and WEBER contrasts, but not with increasing load variability in the VAR contrast (Figure 11C). Similarly, we observed that the transfer function gain ( $b_0$ , ‘effective endpoint compliance’) changed to maintain reach accuracy when the mean load changed in this study. A change in the gain will also effect the zero location (*i.e.* the impulse response) of the adaptation model. However, we observed very little change in the zero location with increasing mean load (MEAN). This was because the influence of previous load ( $b_1$ ) was reduced to balance the gain change. In other words, the relative influence of previous load was found to be invariant with respect to increasing mean load when normalized by the effective limb compliance.

When variability increased (VAR and WEBER), the impulse response of the adaptive process was tuned to reduce transient error through a reduction in zero location. Since changes in effective limb compliance ( $b_0$ ) parallel biomechanical observations, this must be primarily by adjusting the influence of previous load ( $b_1$ ). This demonstrates that subjects adjust the way they integrate information about prior loads into upcoming motor commands to compensate for changes in the overall level of limb impedance required to match changes in the mean stiffness of the environmental load. This suggests that the brain accounts for variations in effective limb compliance in the updating of feedforward motor commands when limb compliance must change to accommodate the load. This suggests that the brain adjusts its information filter properties when adapting to a variable environment.

### ***Reject Weber Equivalency***

The concept of a Weber equivalent contrast arose from the belief that higher order brain regions participate in motor adaptation. To the extent that sensory information processing mechanisms contributing to perception also contribute to motor adaptation and learning, the sensory feedback used to update the next motor command might follow established sensory-perception paradigms demonstrated in the psychophysical literature. Weber's Law states that there is a minimum change in stimulus below which one does not perceive any change. This minimum (called a just noticeable difference or 'jnd') was found to be a constant proportion of the first stimulus intensity. The concept of jnd's was extended by Fechner, who postulated that the jnd was the resolution of sensory-perceptive processes making the relationship between sensation and perception logarithmic (called the Weber-Fechner Principle). By scaling the mean and variability of the load for each block of the WEBER contrast, we intended to compare experimental conditions that were equivalent when interpreted from this logarithmic 'sensory-perception-space'.

Contrary to our original hypothesis, the behavioral results from the WEBER contrast do not support the hypothesis that Weber's Law applies to the sensory information processing underlying motor adaptation. In the WEBER contrast, the mean and variability of the trial-by-trial variation in load were scaled together, which by Weber's Law should result in the perception of similar variability across the blocks of the WEBER contrast. However, we observed changes in subject behavior across the WEBER contrast that paralleled those of the VAR contrast, namely a decrease in the zero location of the motor adaptation model. This finding indicates that we must reject our null hypothesis that motor adaptation adheres to Weber's Law. Liu and Reinkensmeyer (2007) found that subjects will adapt to a viscous curl-field when it is superimposed on a large lateral load that obscured

their ability to perceive the presence and directionality of the viscous curl-field. The loads used in this study were below the jnd threshold since it was demonstrated that subjects could not reliably determine whether the load was half- or full-magnitude or whether it was left- or right-ward in a separate test in the same body of work (Liu and Reinkensmeyer 2007).

Taken together, these findings and our current results suggest that perception and motor control integrate sensory information differently and, thus, Weber's Law is not likely a factor in motor adaptation.

This interpretation may appear to conflict with recent findings that suggest attention plays a role in the processing of sensorimotor memories for motor adaptation (Taylor and Thoroughman 2007). Taylor and Thoroughman (2007) observed unimpaired feedback control within each trial despite the presence of a competing mental task, but noted a reduction in adaptation rate with divided attention. The first finding concurs with previous studies (Allum 1975; Dewhurst 1967; Henry 1953). Dewhurst (1967) demonstrated that subjects exhibited corrective responses in their muscle activity 30 ms after and 50 to 100 ms after the onset of changes in held mass. These response times correspond to monosynaptic and short-loop reflex pathway delays and are much shorter than those of cortical feedback processes, which typically occur around 140 ms (Allum 1975; Dewhurst 1967). Additionally, Henry (1953) demonstrated that subjects made corrections to perturbing forces below their threshold of perceptual detection. However, with regard to the change in adaptation rate, the presence of the competing mental task may have been more than an attention divider, but rather a source for destructive interference in the formation of the internal model necessary for trial-by-trial adaptation (Krakauer et al. 1999; Tong et al. 2002).

### ***Effects of Variability in Other Load Properties***

Fine and Thoroughman (2006 and 2007) have observed that subjects adapt in a manner that is not dependant on perturbation magnitude (i.e. 'categorical adaptation') when perturbations are unpredictable and infrequent. However, their interpretation of load probability differs from that presented here. In their studies, subjects experienced perturbations infrequently (in 20% of trials) and those perturbations varied in magnitude and direction (directed laterally to the left or right), the remaining trials were unperturbed. The infrequency of perturbations creates another source of response variability, specifically, one related to how 'surprising' the perturbation was. There is also a potential for interference due to switching between the two markedly different motor plans required to counter the oppositely directed perturbations (Krakauer et al. 1999; Tong et al. 2002). The infrequent practice and interference would certainly prevent the formation of any relevant internal model, making a proportional adaptation difficult. In fact, Fine and Thoroughman cite the prevention of model formation as the driving design consideration for these types of loads. Without a reliable internal model, subjects would have had to rely primarily on feedback control. We contend that one would see a more robust proportional adaptation in cases where subjects are allowed to establish even a rough internal model. In fact, this was directly observed in both of their studies ((Fine and Thoroughman 2006), Experiment 3; (Fine and Thoroughman 2007), Strong Bias Condition) when the interfering conditions were removed and the practice frequency was increased to 80%.

## CONCLUSIONS AND FUTURE DIRECTIONS

### *Conclusions*

The primary aim of this study was to test the hypothesis that the sensorimotor information processing leading to motor adaptation is sensitive to statistical properties of the environmental load. Our data support this hypothesis. Motor adaptation appears to be sensitive to changes in the trial-by-trial variability of the environmental load. The zero location of the transfer function we used to characterize the process decreased with increasing load variability indicating a trend toward reducing the transient error (or aftereffect) on the following trial(s). Additionally, the feedforward of history information about the load (influence of previous load ( $b_1$ ) in our model) appears to be the driving force behind this change in transient error.

The secondary aim of this work was to test the hypothesis that sensorimotor information processing serving motor adaptation adheres to Weber's Law for sensation. Our data do not support this hypothesis. It was our belief that, if Weber's Law did apply, the load variability across the blocks of the WEBER contrast (simultaneous scaling of mean and standard deviation) would give rise to similar adaptive behavior. However, we observed changes in the zero location of the transfer function we used to characterize motor adaptation similar to those of the increasing variability contrast (VAR).

## ***Future Directions***

In this work we found that subjects adapt to increasing trial-by-trial variability through a decrease in the influence of previous load that leads to a reduction in the transient errors made on future trials. A reduction in the influence of previous perturbation could indicate a shift from predictive control to an adaptive control strategy like muscular co-contraction. A new study could expand on our VAR contrast and incorporate ramp-and-hold perturbations (like those used to estimate limb mechanics in the biomechanics literature) on periodic “probe trials” to assess changes in limb stiffness that would arise from co-contraction of muscles.

Subjects were denied visual feedback of their arm while reaching against the loads in our experimental condition blocks. However, they were provided with timing feedback after each trial. Motor adaptation has been shown to occur without visual feedback (see Background and Significance). However, subjects may have attended more to the timing of their reaches because they received this external feedback and received no external feedback regarding reach extent. In future efforts, we will expand the motor adaptation model to include timing feedback as a regressor to investigate its role in the motor adaptive responses of subjects performing this task.

In addition to timing feedback effects on motor adaptation, it may also be insightful to include additional regressors that reflect the input signals of other sensory systems that could be involved in motor adaptation. Force and position are highly coupled under our experimental conditions due to the use of stiffness loads and a fixed reach distance. As a result, the load stiffness regressors we used will be very similar to the forces measured from the interaction between subjects’ hands and our manipulandum. However, the same Principal Component Analysis technique we used to condense the correlated information

between previous load stiffness ( $K_{i,t}$ ) and previous error ( $\varepsilon_{i,t}$ ) regressors and separate out the remaining uncorrelated signal could be used to separate previous load stiffness and measured force information in a new model. For high stiffness loads, such those used in this work, force may provide a stronger signal to adapt to than proprioception of positional error.

This experiment did not find significant changes in the use of previous extent error in updating future motor commands, although the inter-subject variability of this model parameter was relatively large. It might be possible in a future study to reduce this variability, thus allowing detection of potential changes in this term by adjusting task demands to each subject's strength and range of motion. For example, stiffness loads could be scaled using a measure of the subject's peak force output at MVC. The home position and reach length could also be adjusted such that each subject would move through a similar joint space. The current experimental protocol did not make such accommodations and, in doing so, may have presented varying levels of effort and joint-space motion depending on the limb lengths of each subject.

Finally, the mass and viscosity terms of the perturbing mechanical load were held constant throughout the experiment. However, given the changing stiffness of this system, the damping factor, or general stability, of the mechanical system was not held constant throughout the experiment. This term may be of greater importance to the adapting nervous system since it is a more direct indication of the oscillatory nature (stability) of the perturbing system. Future efforts could revisit this protocol, holding the mass term constant, but tuning the viscosity to the prescribed stiffness to maintain a constant damping factor of the overall perturbing mechanics. This notion of damping factor could also be taken in a different direction. Exposing subjects to several blocks of pseudorandom, trial-by-trial variations in stiffness where each block has a different prescribed damping factor might expose a

relationship between motor adaptation parameters and the overall stability of the mechanical system.

## REFERENCES

- Allum JH. Responses to load disturbances in human shoulder muscles: the hypothesis that one component is a pulse test information signal. *Exp Brain Res* 22: 20, 1975.
- Bays PM, and Wolpert DM. Computational principles of sensorimotor control that minimize uncertainty and variability. *J Physiol* 578: 387, 2007.
- Bock O. Sensorimotor adaptation to visual distortions with different kinematic coupling. *Exp Brain Res* 151: 557-560, 2003.
- Burge J, Ernst MO, and Banks MS. The statistical determinants of adaptation rate in human reaching. *J Vis* 8: 20 21-19, 2008.
- Burke D, McKeon B, and Westerman RA. Induced changes in the thresholds of voluntary activation of human spindle endings. *J Physiol* 302: 11, 1980.
- Conditt MA, Gandolfo F, and Mussa-Ivaldi FA. The motor system does not learn the dynamics of the arm by rote memorization of past experience. *J Neurophysiol* 78: 554-560, 1997.
- Conditt MA, and Mussa-Ivaldi FA. Central representation of time during motor learning. *Proc Natl Acad Sci U S A* 96: 11625-11630, 1999.
- Dewhurst DJ. Neuromuscular control system. *IEEE Trans Biomed Eng* 14: 167-171, 1967.
- Fine MS, and Thoroughman KA. Motor adaptation to single force pulses: sensitive to direction but insensitive to within-movement pulse placement and magnitude. *J Neurophysiol* 96: 710-720, 2006.
- Fine MS, and Thoroughman KA. Trial-by-trial transformation of error into sensorimotor adaptation changes with environmental dynamics. *J Neurophysiol* 98: 1392-1404, 2007.
- Franklin DW, Burdet E, Osu R, Kawato M, and Milner TE. Functional significance of stiffness in adaptation of multijoint arm movements to stable and unstable dynamics. *Exp Brain Res* 151: 145-157, 2003.
- Franklin DW, and Milner TE. Adaptive control of stiffness to stabilize hand position with large loads. *Exp Brain Res* 152: 211-220, 2003.
- Gandevia SC, and Burke D. Effect on voluntary activation of human fusimotor neurons. *J Neurophysiol* 54: 8, 1985.

- Gandevia SC, Wilson LR, Inglis JT, and Burke D. Mental rehearsal of motor tasks recruits alpha-motoneurons but fails to recruit human fusimotor neurons selectively. *J Physiol* 505: 8, 1997.
- Gescheider G. *Psychophysics: Method, Theory, and Application*. New Jersey: Lawrence Erlbaum Associates, 1985, p. 295.
- Gomi H, and Osu R. Task-Dependent Viscoelasticity of Human Multijoint Arm and Its Spatial Characteristics for Interaction with Environments. *J Neurosci* 18: 8965, 1998.
- Granit, R. The functional role of the muscle spindles - facts and hypotheses. *Brain* 98, 531-556, 1975.
- Guyton A, and Hall J. *Textbook of medical physiology*. Philadelphia: W.B. Saunders Company, 2000.
- Hanaford B, Lakshminarayanan V, Stark L, and Nam M. Electromyographic evidence of neurological controller signals with viscous load. *J Mot Behav* 16(3): 255, 1984.
- Henry F. Dynamic kinesthetic perception and adjustment. *Res Q* 11, 1953.
- Hulliger M, and Prochazka A. A new simulation method to deduce fusimotor activity from afferent discharge recorded in freely moving cats. *J Neurosci Meth* 8, 197-204, 1983.
- Judkins T. Visual and proprioceptive contributions to adaptation of the human reach. In: *Biomedical Engineering*. Milwaukee: Marquette University, 2004.
- Kakuda N, Wessberg J, and Vallbo AB. Is human muscle spindle afference dependent on perceived size of error in visual tracking? *Exp Brain Res* 114: 9, 1997.
- Kirsch RF, and Rymer WZ. Neural compensation for fatigue-induced changes in muscle stiffness during perturbations of elbow angle in human. *J Neurophysiol* 68: 449-470, 1992.
- Kirsch RF, and Rymer WZ. Neural Compensation for Muscular Fatigue: Evidence for Significant Force Regulation in Man. *J Neurophysiol* 57: 18, 1987.
- Kording KP, Tenenbaum JB, and Shadmehr R. The dynamics of memory as a consequence of optimal adaptation to a changing body. *Nature Neurosci* 10: 779-786, 2007.
- Korenberg AT, and Ghahramani Z. A Bayesian view of motor adaptation. *Current Psychology of Cognition* 21: 537, 2002.
- Krakauer J, Ghilardi M, and Ghez C. Independent learning of internal models for kinematic and dynamic control of reaching. *Nature Neurosci* 2: 1026-1031, 1999.

- Krakauer JW, Mazzoni P, Ghazizadeh A, Ravindran R, and Shadmehr R. Generalization of Motor Learning Depends on the History of Prior Action. *PLoS Biol* 4: e316, 2006.
- Lai EJ, Hodgson AJ, and Milner TE. Influence of interaction force levels on degree of motor adaptation in a stable dynamic force field. *Exp Brain Res* 153: 76-83, 2003.
- Liu J, and Reinkensmeyer DJ. Motor adaptation to a small force field superimposed on a large background force. *Exp Brain Res* 178: 402-414, 2007.
- Ljung L. *System Identification - Theory for the user*. Englewood Cliffs, NJ: Prentice Hall, 1999.
- Lund RE. Tables for An Approximate Test for Outliers in Linear Models. *Technometrics* 17: 473-476, 1975.
- Matlin M, and Foley H. *Sensation and Perception*. Boston: Allyn and Bacon, 1997, p. 554.
- Maybeck P. *Stochastic models, estimation, and control*. Academic Press, 1979.
- Patton J, and Mussa-Ivaldi F. Robot-Assisted Adaptive Training: Custom Force Fields for Teaching Movement Patterns. *IEEE Trans Biomed Eng* 51: 636-646, 2004.
- Perreault EJ, Kirsch RF, and Crago PE. Multijoint dynamics and postural stability of the human arm. *Exp Brain Res* 157: 507-517, 2004.
- Prochazka A, Hulliger M, Zangger P, and Appenteng K. Fusimotor set: new evidence for a-independent control of g-motoneurons during movement in the awake cat. 339: 136-140, 1985.
- Sainburg RL, Ghez C, and Kalakanis D. Intersegmental Dynamics Are Controlled by Sequential Anticipatory, Error Correction, and Postural Mechanisms. *J Neurophysiol* 81: 12, 1999.
- Scheidt R. A vector-ARX model of motor adaptation during reaching. In: *Advances in Computational Motor Control III*. SanDiego, CA: Society for Neuroscience, 2004.
- Scheidt RA, Conditt MA, Secco EL, and Mussa-Ivaldi FA. Interaction of visual and proprioceptive feedback during adaptation of human reaching movements. *J Neurophysiol* 93: 3200-3213, 2005.
- Scheidt RA, Dingwell JB, and Mussa-Ivaldi FA. Learning to move amid uncertainty. *J Neurophysiol* 86: 971-985, 2001.
- Scheidt RA, Reinkensmeyer DJ, Conditt MA, Rymer WZ, and Mussa-Ivaldi FA. Persistence of Motor Adaptation During Constrained, Multi-Joint, Arm Movements. *J Neurophysiol* 84: 853-862, 2000.

- Scheidt RA, and Stoeckmann T. Reach Adaptation and Final Position Control Amid Environmental Uncertainty Following Stroke. *J Neurophysiol* 2007.
- Takahashi CD, Nemet D, Rose-Gotttron CM, Larson JK, Cooper DM, and Reinkensmeyer DJ. Effect of muscle fatigue on internal model formation and retention during reaching with the arm. *J Appl Physiol* 100: 695-706, 2006.
- Taylor JA, and Thoroughman KA. Divided attention impairs human motor adaptation but not feedback control. *J Neurophysiol* 98: 317-326, 2007.
- Thoroughman KA, and Shadmehr R. Learning of action through adaptive combination of motor primitives. *Nature* 407: 742-747, 2000.
- Thurstone LL. Psychophysical Analysis. 38: 368-389, 1927.
- Todorov E. Stochastic Optimal Control and Estimation Methods Adapted to the Noise Characteristics of the Sensorimotor System. *Neural Computation* 17: 1084-1108, 2005.
- Tong C, Wolpert DM, and Flanagan JR. Kinematics and Dynamics Are Not Represented Independently in Motor Working Memory: Evidence from an Interference Study. *J Neurosci* 22: 1108-1113, 2002.
- Weber EH, *The sense of touch*. Ross, HE and Murray, DJ (Translators). Academic Press, London, 1978.
- Weeks DL, Aubert MP, Feldman AG, and Levin MF. One-trial adaptation of movement to changes in load. 75: 60-74, 1996.
- Wei K, and Kording K. Relevance of error: what drives motor adaptation? *J Neurophysiol* 101: 655-664, 2009.
- Welch G, and Bishop G. *An Introduction to the Kalman Filter*. Dept. Comp. Sci., Univ. North Carolina, Chapel Hill, TR 95-041, 2006.
- Wolpert DM. Probabilistic models in human sensorimotor control. *Hum Mov Sci* 26: 511-524, 2007.